Master's Thesis
석사 학위논문

Regulation of stress-evoked behaviors by astrocytes in the lateral septum

Yeonju Sin(신 연 주 申 娟 周)

Department of
Brain and Cognitive Sciences

DGIST

2021

Master's Thesis
석사 학위논문

Regulation of stress-evoked behaviors by astrocytes in the lateral septum

Yeonju Sin(신 연 주 申 娟 周)

Department of
Brain and Cognitive Sciences

DGIST

2021

Regulation of stress-evoked behaviors by astrocytes in the lateral septum

Advisor: Professor Hyosang Lee
Co-advisor: Professor Yong-Seok Oh

By

Yeonju Sin
Department of Brain and Cognitive Sciences
DGIST

A thesis submitted to the faculty of DGIST in partial fulfillment of the requirements for the degree of Master of Science in the Department of Brain and Cognitive Sciences. The study was conducted in accordance with Code of Research Ethics[1].

06. 25. 2021

Approved by

Professor Hyosang Lee (signature)
(Advisor)

Professor Yong-Seok Oh (signature)
(Co-Advisor)

[1] Declaration of Ethical Conduct in Research**:** I, as a graduate student of DGIST, hereby declare that I have not committed any acts that may damage the credibility of my research. These include, but are not limited to: falsification, thesis written by someone else, distortion of research findings or plagiarism. I affirm that my thesis contains honest conclusions based on my own careful research under the guidance of my thesis advisor.

Regulation of stress-evoked behaviors by astrocytes in the lateral septum

Yeonju Sin

Accepted in partial fulfillment of the requirements for the degree of Master of Science.

06. 25. 2021

Head of Committee	Prof. Hyosang Lee	(signature)
Committee Member	Prof. Yong-Seok Oh	(signature)
Committee Member	Prof. Han Kyoung Choe	(signature)

MS/BS
201925006

신 연 주. Yeonju Sin. Regulation of stress-evoked behaviors by astrocytes in the lateral septum. Department of Brain and Cognitive Sciences. 2021. 58p. Advisors Prof. Hyosang Lee, Co-Advisors Prof. Yong-Seok Oh

ABSTRACT

Chronic stress has been implicated in anxiety, depression, and other mental disorders. In this regard, studies on the neural mechanism mediating behavioral response to stress have been mainly progressed, but in recent years there has been a growing interest of studying astrocytes. Astrocytes not only provide homeostatic support for neurons but also play an important role in behavioral regulation by interacting with neurons. However, despite the diverse functions of astrocytes, research focusing on the role of astrocytes in stress-induced behaviors has been conducted in only a few brain regions. Using chronic social defeat stress (CSDS), an animal model for depression, we found that astrocytes in the lateral septum (LS) area exhibited a delayed response to CSDS. Specifically, molecular and morphological changes, indicating reactive astrocytes, were observed in the LS after CSDS. Raising astrocytic calcium signaling by Gq pathway activation in LS astrocytes stimulated astrocytes and nearby neurons and promoted depressive- and anxiety-like behaviors under subthreshold stress that did not alter behaviors in unmanipulated mice. In contrast, reducing calcium signaling in LS astrocytes blocked acute stress-induced neuronal activity. Notably, selective inhibition of LS astrocytes was sufficient to produce antidepressant-like effects following CSDS. These findings suggest that astrocytes in the LS may contribute to regulating stress-evoked behaviors and providing a novel therapeutic target for treating depression.

Keywords: stress, astrocytes, lateral septum, depression, anxiety, social defeat, chemogenetics, cFos

List of Contents

List of Figures

I. INTRODUCTION

Maladaptive response to environmental stress is a risk factor for psychiatric diseases, including depression and anxiety (Caspi, 2003; Bartolomucci and Leopardi, 2009; Heim and Nemeroff, 2001). Repeated and prolonged exposure to noxious stimuli impairs behavioral responsiveness and increases susceptibility to mental disorders (Mariotti, 2015; Chaijale et al., 2014). To date, the mechanisms underlying stress-induced behavioral dysfunction have been largely studied by using animal models. In rodent models, chronic social defeat stress (CSDS) is considered as one of the robust models for studying stress-induced mood disorders due to its etiological relevance and similarity to psychosocial stress experienced by humans (Berton et al., 2006; Golden et al., 2011). Social defeat stress increases activation of the hypothalamic-pituitary-adrenal (HPA) axis and elevates levels of blood serum corticosterone (Buwalda et al., 1999). Additionally, it induces social avoidance, dysfunctional reward-related behaviors, and increased sensitivity to helplessness measures which are described as depressive-like symptoms (Krishnan and Nestler, 2008; Kudryavtseva et al., 1991).

The neural mechanisms regulating responses to CSDS have been well-characterized, especially concerning cellular and molecular adaptations in the mesolimbic dopamine system. Following CSDS, brain-derived neurotrophic factor (BDNF) expression is increased in the nucleus accumbens (NAc) of susceptible mice, and local knockdown of BDNF in dopaminergic neurons from the ventral tegmental area (VTA) blocks SDS-induced social avoidance (Berton et al., 2006). Susceptible mice also show an upregulation of phasic firing in VTA dopamine neurons, an effect not seen in resilient mice (Krishnan et al., 2007). When the VTA-NAc pathway is optogenetically stimulated, susceptible phenotypes are rapidly induced in mice previously resistant to the effects of CSDS, whereas optoge-

netic inhibition of this pathway induces resilience (Chaudhury et al., 2012). In addition, recent evidence shows that CSDS reduces levels of neuroligin 2, the inhibitory synapse-specific protein, in the NAc medium spiny neurons (MSNs), which promotes social avoidance (Heshmati et al., 2018).

Although evidence for underlying neural circuits of SDS-induced behaviors has been presented in many researches, few studies have directly assessed the contribution of non-neuronal cells to the development of those behaviors. Astrocytes, the most abundant non-neuronal cells found in the central nervous system, have traditionally been considered as supportive cells supplying energy sources to neurons, providing homeostasis control, and maintaining the blood-brain barrier (Tian et al., 2005; Tsacopoulos and Magistretti, 1996; Janzer and Raff, 1987; Parpura and Verkhratsky, 2012). Astrocytes have also been found to sense and affect neuronal excitability, synaptic plasticity, and the local environment with an intracellular calcium transient (Haim and Rowitch, 2016; Nagai et al., 2019; Panatier et al., 2011). When the intracellular calcium level is increased in response to neurotransmitters, astrocytes release neuroactive substances, termed “gliotransmitters”, that regulate synaptic transmission and plasticity (Perez-Alvarez et al., 2014; Guerra-Gomes et al., 2018). Accumulating data suggest that astrocytes are involved in neuronal circuit functions and regulate various behaviors, including learning and memory, fear response, and depression-related behaviors (Adamsky et al., 2018; Cao et al., 2013; Martin-Fernandez et al., 2017; Nam et al., 2019).

Several postmortem studies have reported that individuals have suffered from major depressive disorder (MDD) showed alterations of astrocytic characters, such as cell number and density, morphology, protein expression level, and membrane channel functions in the different brain regions including the medial prefrontal cortex, hippocampus, amygdala, and locus coeruleus (Bernard et al.,

2010; Bowley et al., 2002; Chandley et al., 2013; Choudary et al., 2005; Cotter et al., 2002; Ernst et al., 2011; Klempan et al., 2007; Miguel-Hidalgo et al., 2014; Rajkowska et al., 1999). For example, gene transcription and protein expression of a glial fibrillary acidic protein (GFAP), the main intermediate filament in astrocytes, decreased in various brain regions (Altshuler et al., 2010; Chandley et al., 2013; Miguel-Hidalgo et al., 2010; Müller et al., 2001; Torres-Platas et al., 2015). Other studies have also reported increased astrocytic cell density in hippocampal regions and hypertrophy of astrocytes in the white matter of the anterior cingulate cortex of depressive patients (Stockmeier et al., 2004; Torres-Platas et al., 2011). In addition to the studies on humans, those using rodents have also revealed that astrocytes have functionally crucial roles in depression. By way of illustration, astrocytic lesions, but not neuronal lesions, of the prefrontal cortex is sufficient to trigger depressive- and anxiety-like phenotypes (Banasr and Duman, 2008). Lastly, a recent study showing that astrocytes can induce depressive symptoms by producing pro-inflammatory cytokines and interacting with neurons suggests astrocytes as promising targets for regulating depression (Leng et al., 2018). However, despite the heterogeneity of region-specific astrocytic functions, studies on the role of astrocytes in depression have been conducted in only a few brain areas.

Here, we identified that astrocytes in the lateral septum (LS) respond to chronic social defeat stress (CSDS), which results in increased astrocytic activity and altered morphology. To explore the role of LS astrocytes in modulating behavioral responses to social defeat stress, astrocyte-specific chemogenetic tools were employed. Neither acute nor chronic activation of LS astrocytes was sufficient to trigger behavioral changes in stress-naïve mice, but astrocytic activation combined with subthreshold social defeat stress enhanced depression- and anxiety-like behaviors. Moreover, reducing

calcium signaling in LS astrocytes rescued depression-like behaviors following CSDS. Taken together, this study shows that the LS astrocytes can regulate stress-evoked behaviors, suggesting a potential therapeutic target for the treatment of stress-induced disorders.

II. MATERIALS & METHODS

Animals

All animal experiments were approved by the Institutional Animal Care and Use Committee at the Daegu Gyeongbuk Institute of Science & Technology (DGIST-IACUC-20011502-08) and conducted in accordance with NIH guidelines. Wildtype C57BL/6J mice (C57BL/6JBomTac) and CD1 retired breeders were purchased from a vendor (DBL, South Korea). Two to five mice were housed per cage and maintained on a 12-h light/dark schedule with *ad libitum* access to food and water. C57BL/6J mice at the age of 8 to 14 weeks were housed singly at least seven days before being tested behaviorally or imposed on social defeat stress. CD1 male mice aged over three months were used as aggressors in the social defeat stress model.

Virus

Viruses were purchased from the Viral Vector Facility (VVF) at the University of Zürich (AAV5-hgfaABC1D-hM3Dq-mCherry, 6.0×10^{12} gc/ml; AAV5-hgfaABC1D-mCherry, 6.1×10^{12} gc/ml; AAV5-hgfaABC1D-EGFP, 7.0×10^{12} gc/ml). AAV5-GfaABC1D-mCherry-hPMCA2w/b (7.1×10^{12} gc/ml) was packaged at the University of Pennsylvania Vector Core using a viral vector purchased from Addgene (pZac2.1-GfaABC1D-mCherry-hPMCA2w/b).

Stereotaxic surgery

A virus was injected into a target brain region using stereotaxic surgery, as described previously (Lee et al., 2014). Briefly, a mouse was acutely anesthetized in an induction chamber infused with 2.5%

isoflurane mixed with oxygen and then quickly positioned in a stereotaxic frame, in which 1-2.5% anesthetizing gas was continuously infused to the mouse nose through a nosecone (David Kopf Instruments). After lubricating eyes with Liposic ophthalmic gel (Bausch & Lomb), an incision was made in the scalp, and a hole was drilled in the skull above the target brain region. 50-100 nl of viral solution loaded in a pulled glass capillary (World Precision Instruments) was injected into the LS at the speed of 20-30 nl per min using Nanoliter Injector (World Precision Instruments) and Micoro4 controller (World Precision Instruments). The injection coordinates were obtained from either the Paxinos and Franklin's the Mouse Brain in Stereotaxic Coordinates (ML: ±0.39; AP: -0.05; DV: -2.5 mm) or the three-dimensional surgical atlas of the murine head based on magnetic resonance imaging and micro-computed tomography (ML: ±0.39; AP: -3.39; DV: -2.2 mm) (Chan et al., 2007). After closing the incision in the scalp with a tissue-adhesive bond (Vetbond, 3M), the mouse was injected intraperitoneally with ketoprofen (2 μg/g, Unibio) and returned to its home cage. Ibuprofen (0.2 mg/ml, Hanmi Pharm) was provided in drinking water more than three days after the surgery.

Behavioral tests

All behavioral tests were carried out during the light period of the day. Scoring of animal behavior was conducted by investigators blind to treatments.

Clozapine N-Oxide (CNO) administration

CNO (3 mg/kg, Enzo Lifesciences) dissolved in 0.9% NaCl was administered to a mouse intraperitoneally 30 min before the beginning of each behavioral test or imposing the social defeat stress. For

the chronic activation of hM3Dq expressed in astrocytes, mice were injected intraperitoneally with CNO (3 mg/kg) for ten consecutive days at 9-10 AM. The concentration of CNO used in this study caused no detectable behavioral side effects in control animals.

Chronic social defeat stress (CSDS)

Chronic social defeat stress was applied to C57BL/6J male mice, as previously described (Golden et al., 2011). Aggressor mice were selected from vendor-bought CD1 male retired breeders with the following criteria: exhibiting at least one attack episode towards C57BL/6J male intruders in more than two out of three 5-min screening sessions and less than 90 s average attack latency in three screening sessions. A subject C57BL/6J male mouse was introduced into the home cage of a pre-screened CD1 aggressor to receive physical attacks for 5-10 min. The subject and aggressor mice stayed in the same cage, but in different compartments separated by a perforated plexiglass divider for 24 hours. The whole session was repeated in ten consecutive days by introducing a novel CD1 aggressor in each session. In the control group, a subject mouse stayed with a conspecific male mouse for 24 hours in separate compartments of a cage divided by a perforated plexiglass barrier in the middle. The session was repeated for ten consecutive days by using a novel conspecific male mouse in each session. Both control and socially defeated C57BL/6J mice were then subjected to the social interaction test performed on the next day.

Subthreshold social defeat stress (SSDS)

Subthreshold social defeat stress was given to C57BL/6J male mice, as previously described

(Chaudhury et al., 2012; Shen et al., 2019). A subject male mouse was placed into the home cage of a pre-screened CD1 aggressor to receive attacks for 10 min. The subject and aggressor mice then stayed in the same cage, but in different compartments divided by the perforated plexiglass barrier built in the middle of the cage for another 10 min. The subject mouse was returned to its home cage for 5 min. Then, the whole session was repeated once more using a novel aggressor. CNO (3 mg/kg) was injected intraperitoneally into the subject mouse 20 min before the beginning of SSDS. At the end of the second session, the subject mouse was returned to its home cage and housed individually until the social interaction test performed on the next day.

Social interaction test

The social interaction test was performed as previously described (Golden et al., 2011; Berton et al., 2006). In the initial session ("no target"), a subject C57BL/6J male mouse was placed in a 38.8 cm (width and length) × 33.9 cm (height) test box containing an empty 10.5 cm (diameter) × 23 cm (height) wire-mesh enclosure on one side of the box. Mouse behavior was recorded with a video camera on the ceiling for 150 s. In the immediately following session ("target"), a novel CD1 mouse that the subject never encountered previously was placed inside the wire-mesh enclosure, and then the subject mouse was re-introduced into the test box. Mouse behavior was recorded for 150 s. The brightness of the test room was less than 5 lux for both sessions. The amount of time mouse spent in the interaction zone, which is 7.39 cm around the wire mesh enclosure, was calculated using Ethovision XT 11.5.

Open field test

A mouse was placed in the middle of a 38.8 cm (width and length) × 34 cm (height) test box. Mouse behavior was recorded with a video camera on the ceiling for 10 min. The brightness of the test room was 60 lux. The amount of time mouse spent in the center zone (23.28 cm in width and length) was analyzed using Ethovision XT 11.5.

Elevated plus maze test

The elevated plus maze apparatus was composed of two 30.5 cm (width) × 6.0 cm (length) open arms (150 lux) and two closed arms by the same size, but with 25 cm height walls around the arms (50 lux). The arms were positioned 50 cm from the floor. A mouse was placed in the center zone and allowed to explore for 5 min. Mouse behavior was recorded with a video camera on the ceiling. The amount of time mouse spent in the open arms was analyzed using Ethovision XT 11.5.

Forced swim test

A mouse was released into a 12 cm (diameter) × 28 cm (height) glass cylinder containing water (23 ± 1°C) filled up to 13 cm. Mouse behavior was recorded for 6 min using a webcam, and the last 4 min was used for analysis. The amount of time the mouse exhibited immobility was calculated by subtracting the amount of time the mouse exhibited movements except for those necessary for balancing the body and keeping the head out of the water from the 4-min test duration (Cryan et al., 2002).

Histology

Mice were anesthetized by injecting 2% avertin and perfused transcardially with 20 ml phosphate-buffered saline (PBS), followed by 20 ml ice-cold 4% paraformaldehyde (Sigma Aldrich) in PBS. The brain was dissected out and cryoprotected in 30% sucrose for 48 hours at 4°C. Then, the brain was frozen in optimum cutting temperature compound (Scigen) and stored at -80°C. Brain sections were cut to 30 μm in thickness using a cryostat (CM3050 S, Leica).

For detecting cFos expression following activation of hM3Dq in LS astrocytes or social defeat stress, a mouse was injected intraperitoneally with CNO (3 mg/kg) or exposed to a pre-screened CD1 aggressor and then perfused with 4% paraformaldehyde. The rest procedures are described above.

Immunohistochemistry

Sections were incubated in blocking solution (5% normal donkey serum in PBS containing 0.3% Triton X-100, NDST) for one hour at room temperature and then treated with primary antibodies diluted in 1% NDST at 4°C overnight. The following day, the sections were rinsed with 0.3% Triton X-100 in PBS three times for 5 min each and subsequently incubated with secondary antibodies diluted in 1% NDST for two hours at room temperature. The primary antibodies are rabbit anti-GFAP (1:500, Z0334, DAKO), rabbit anti-cFos (1:300, 2250, Cell signaling), mouse anti-NeuN (1:500, MAB377, Millipore), and chicken anti-NeuN (1:500, ABN91, Millipore). The secondary antibodies are Alexa Fluor 488 donkey anti-rabbit (1:500, A21206, Life tech.), Alexa Fluor 647 donkey anti-rabbit (1:500, A31573, Life tech.), Alexa Flour 488 donkey anti-mouse (1:500, A21202, Life tech.), and Alexa Flour 649 donkey anti-chicken (1:500, A11057, Jackson ImmunoResearch). Lastly, DAPI (1:1000, D9542, Sigma-Aldrich) was used for nuclei staining.

Image quantification

Fluorescent images were acquired using the slide scanner (Axio Scan Z1, Carl Zeiss) and confocal microscope (LSM 700, LSM 800, Carl Zeiss). The mean intensity of GFAP immunoreactivities in the LS were measured using ZEN 2 (Carl Zeiss) and ImageJ. The number of $cFos^+$ and $NeuN^+$ cells in five sequential segments of the LS along the anterior to posterior axis was analyzed using ImageJ. For three-dimensional (3D) reconstructions, serial confocal images of GFAP sections were analyzed with Imaris software (Bitplane).

Statistical analysis

Data are expressed as mean ± S.E.M (*n* = number of animals or samples). Data from behavioral experiments were evaluated statistically using the Mann-Whitney U test and repeated measure one- or two-way ANOVA with Bonferroni post hoc corrections. Histological data were analyzed using two-tailed t-tests. Statistical analyses were performed using Microsoft Excel or Prism (GraphPad). $P < 0.05$ was considered to be significant.

III. RESULTS

3.1 Chronic social defeat stress increases astrocytic activity in the lateral septum.

Chronic social defeat stress (CSDS) is a well-established mouse model which causes robust and long-lasting behavioral phenotypes related to social avoidance, depression, and anxiety in male mice (Berton et al., 2006; Golden et al., 2011; Kudryavtseva et al., 1991; Rygula et al., 2006). To validate behavioral symptoms in this model, mice were subjected to social defeat stress for 10 consecutive days and underwent behavior assays including social interaction (SI) test, forced swim (FS) test, open field (OF) test, and elevated plus maze (EPM) test (Fig. 1A). As previously reported, defeated mice showed decreased time in the interaction zone during the target session in the SI test compared to control mice (Fig. 1B, C). In the FS test, CSDS caused increased immobility time in mice (Fig. 1D). In addition, defeated mice spent significantly less time in the center area of the OF (Fig. 1E) and the open arms of the EPM (Fig. 1F) than control mice. Thus, CSDS results in depression- and anxiety-like behaviors in mice.

To assess whether astrocytes are involved in depressive- and anxiety-like behaviors induced by CSDS, we examined the expression of astrocyte-specific activity marker, glial fibrillary acidic protein (GFAP) in the entire mouse brain after CSDS (Fig. 2A). The time-course analysis revealed that GFAP expression is unchanged after 1 day of CSDS (D11), but significantly increased at 7 days post-CSDS (D17) in the lateral septum (LS) area of the defeated mice (Fig. 2B, C, D, E). Histological quantification performed at D38 further revealed that the increase of GFAP expression induced by CSDS was observed even on the 28 days post-CSDS, a period during which defeat-induced social avoidance is maintained (Fig. 2F, G).

Astrocytes are morphologically complex cells that have a soma, several major branches, and numerous fine processes that contact diverse cellular elements (Haim and Rowitch, 2016; Schiweck et al., 2018). Moreover, astrocytes are known to alter their morphology during development or physiological conditions (Sun et al., 2017; Naskar and Chattarji, 2019). Thus, morphological analysis of astrocytes is necessary to understand astrocyte function. To further investigate morphometric changes caused by CSDS in the LS, we performed a Sholl analysis of individually 3D-reconstructed astrocytes using Imaris analysis software (Fig. 2H). After CSDS, astrocytes in the LS of the defeated mice showed an increase in number and total length of astrocytic processes, without altered mean dendrite length (Fig. 2I, J, K). The number of dendritic intersections occurring at a circle starting from the center of the soma with a 1 μm increase in radius was also increased in the defeated group (Fig. 2L). Together, these results suggest that astrocytes in the LS are activated by CSDS, displaying features of reactive astrocytes indicated by increased GFAP expression and morphological complexity.

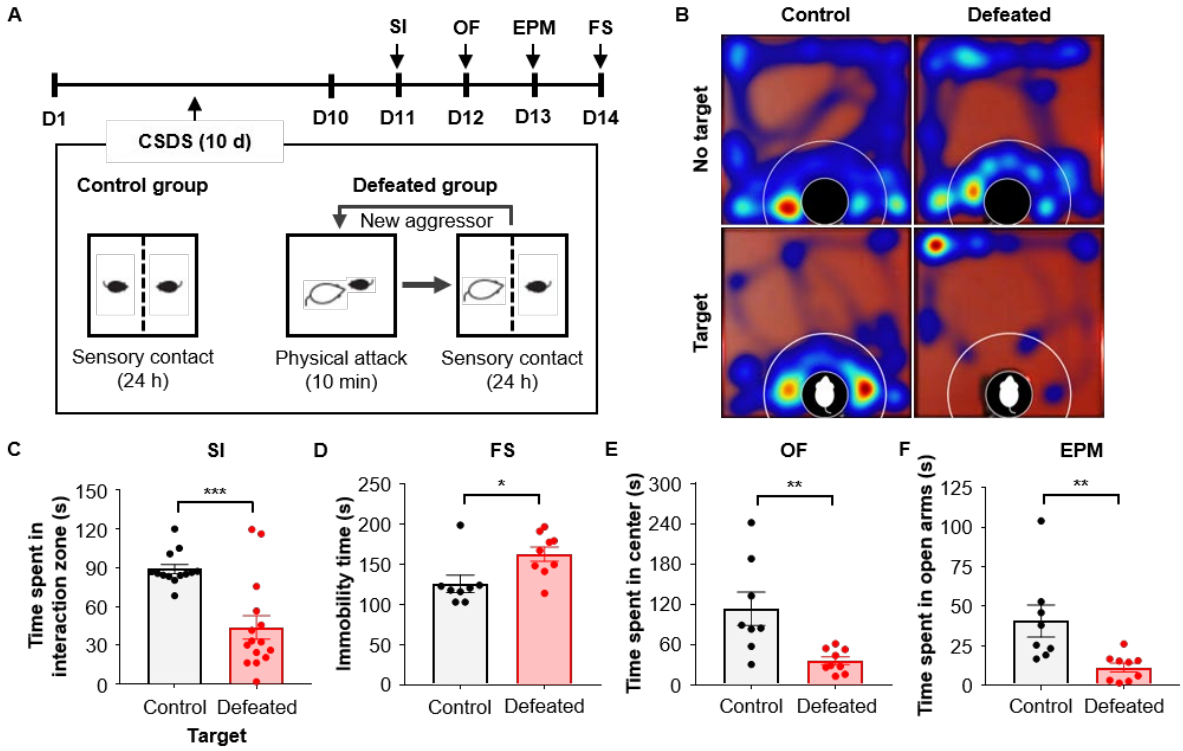
A
SI
OF
EPM
FS
D1
D10
D11
D12
D13
D14
CSDS (10 d)
Control group
Defeated group
New aggressor
Sensory contact
(24 h)
Physical attack
(10 min)
Sensory contact
(24 h)
B
Control
Defeated
No target
Target
C
SI
Time spent in interaction zone (s)
***
Control
Defeated
Target
D
FS
Immobility time (s)
*
Control
Defeated
E
OF
Time spent in center (s)
**
Control
Defeated
F
EPM
Time spent in open arms (s)
**
Control
Defeated

Figure 1. Chronic social defeat stress causes depressive- and anxiety-like behaviors in mice.

(A) Schematic representation of CSDS procedure and timeline of behavioral tests. (B) Heat maps indicating time spent in the chamber of social interaction test for example control and defeated mice. (C) Time spent in the interaction zone during the target session of SI test (Mann-Whitney test, p=0.0004; control n=13, defeated n=15). (D) Immobility time in FS test (Mann-Whitney test, p=0.0360; control n=8, defeated n=9). (E) Time spent in the center zone of OF test (Mann-Whitney test, p=0.0016; control n=8, defeated n=9). (F) Time spent in the open arms of EPM test (Mann-Whitney test, p=0.0016; control n=8, defeated n=9). Data are represented as mean ± S.E.M. *p < 0.05, **p < 0.01, ***p < 0.001.

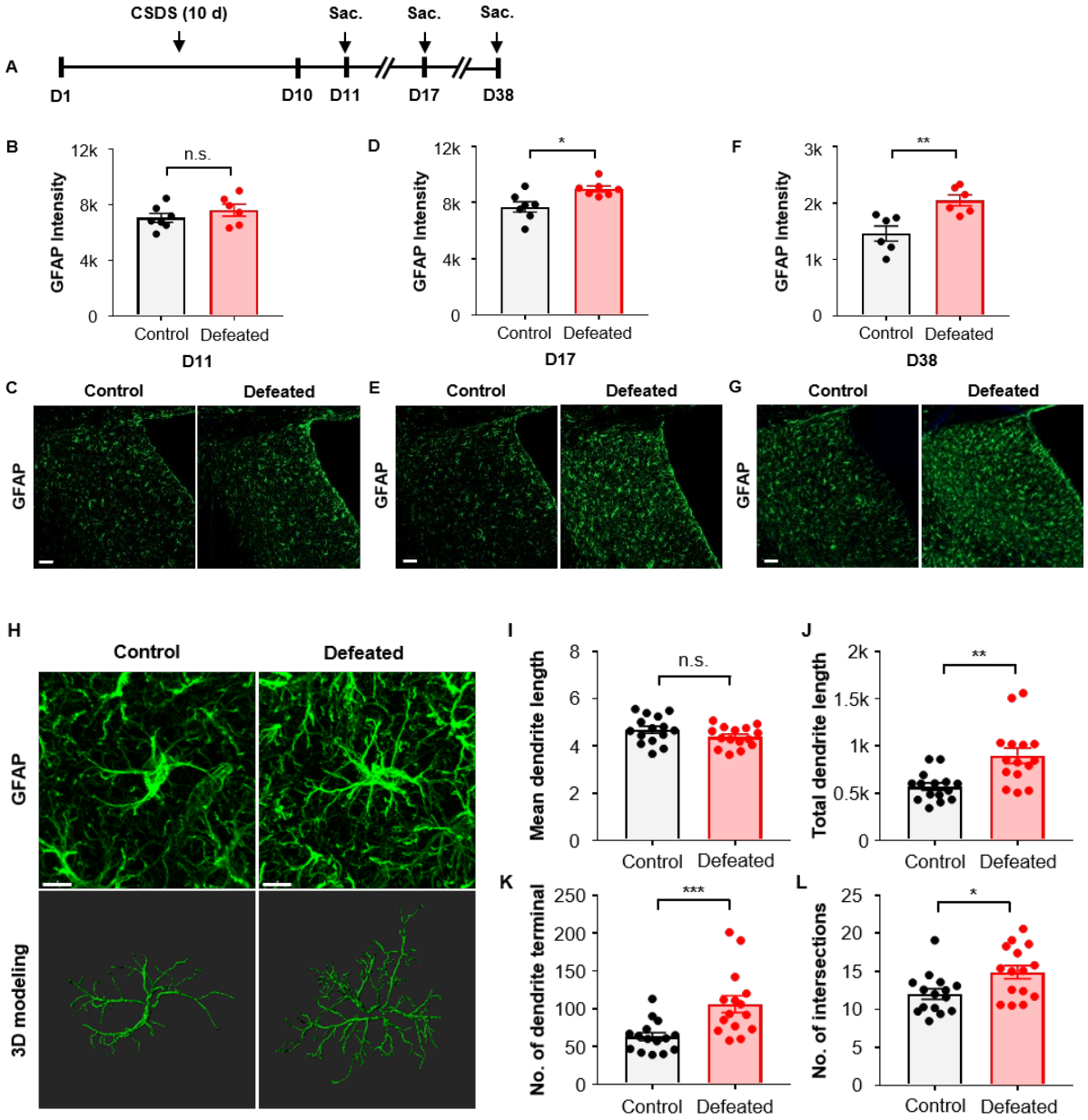
A
CSDS (10 d)
Sac.
Sac.
Sac.
D1
D10
D11
D17
D38
B
GFAP Intensity
12k
8k
4k
0
n.s.
Control
Defeated
D11
D
*
D17
F
**
3k
2k
1k
D38
C
Control
Defeated
GFAP
E
G
H
3D modeling
I
Mean dendrite length
8
6
4
2
J
Total dendrite length
2k
1.5k
1k
0.5k
K
No. of dendrite terminal
250
200
150
100
50
***
L
No. of intersections
25
20
15
10
5

Figure 2. Chronic social defeat stress induces delayed molecular and morphological changes of astrocytes in the lateral septum.

(A) Schematic of experimental timeline. (B) Quantification of GFAP intensity in the LS on D11 (Unpaired t test, p=0.3139; control n=7, defeated n=6). (C) Representative images of GFAP expression in the LS of control (left) or defeated (right) mice on D11. Scale bars: 50 μm. (D) Quantification of GFAP intensity in the LS on D17 (Unpaired t test, p=0.0107; control n=7, defeated n=7). (E) Representative images of GFAP expression in the LS of control (left) or defeated (right) mice on D17. Scale bars: 50 μm. (F) Quantification of GFAP intensity in the LS on D38 (Unpaired t test, p=0.0049; control n=7, defeated n=7). (G) Representative images of GFAP expression in the LS of control (left) or defeated (right) mice on D38. Scale bars: 50 μm. (H) Representative images of GFAP-stained astrocytes (up) and 3D-rendered astrocytes using Imaris (down) in the LS of control (left) or defeated (right) mice on D38. Scale bars: 8 μm. (I) Average length of dendrites from astrocytes in the LS (Unpaired t test, p=0.1159; 15 cells from 5 mice from each group). (J) Total dendrite length of astrocytes in the LS (Unpaired t test, p=0.0011; 15 cells from 5 mice from each group). (K) The number of dendrite terminals of astrocytes in the LS (Unpaired t test, p=0.0017; 15 cells from 5 mice from each group). (L) The number of intersections of astrocytes in the LS by Sholl analysis (Unpaired t test, p=0.0149; 15 cells from 5 mice from each group). Data are represented as mean ± S.E.M. *p < 0.05, **p < 0.01, ***p < 0.001; n.s., not significant.

3.2 Gq pathway activation in LS astrocytes is sufficient to modulate astrocytic and neuronal activity.

If heightened activity of astrocytes is a characteristic of CSDS-induced changes in the LS, we hypothesized that artificially increasing the activity of LS astrocytes could mimic molecular and behavioral changes evoked by CSDS. To achieve this, we employed Gq-coupled human Gq-coupled M3 muscarinic receptor (hM3Dq) to activate LS astrocytes with its agonist clozapine-N-oxide (CNO) since endogenous Gq-coupled GPCRs are primarily involved in the astrocytic calcium signaling and astrocyte-neuron interaction (Agulhon et al., 2008; Araque et al., 2014; Guerra-Gomes et al., 2018). To validate the efficacy of chemogenetic activation of the astrocytes in vivo, an adeno-associated virus serotype 5 (AAV5) vector encoding hM3Dq fused to mCherry under the control of the astrocytic hgfaABC1D promoter (AAV5-hgfaABC1D-hM3Dq-mCherry) was delivered to the LS region (Fig. 3A). The hgfaABC1D promoter, a compact GFAP promoter, was used in this study since it showed high transduction efficiency in the previous study (Griffin et al., 2019). Co-staining with the astrocytic marker GFAP and the neuronal marker NeuN showed that the virus expression was found exclusively in astrocytes (> 95% of the GFAP cells expressed hM3Dq), but not in neurons (Fig. 3B).

To verify that hM3Dq activates astrocytes upon CNO application, CNO (3 mg/kg) or saline was administered intraperitoneally to the mice and the brains were collected for histological analysis 90 min after drug injection (Fig. 3A). CNO increased the GFAP expression in LS astrocytes of compared with saline-injected controls (Fig. 4A, B). Moreover, hM3Dq activation with CNO also increased the number of cFos-positive neurons in the LS (Fig. 4C, D). These data suggest that Gq pathway activation in astrocytes increases astrocytic activity and nearby neuronal activity in the LS.

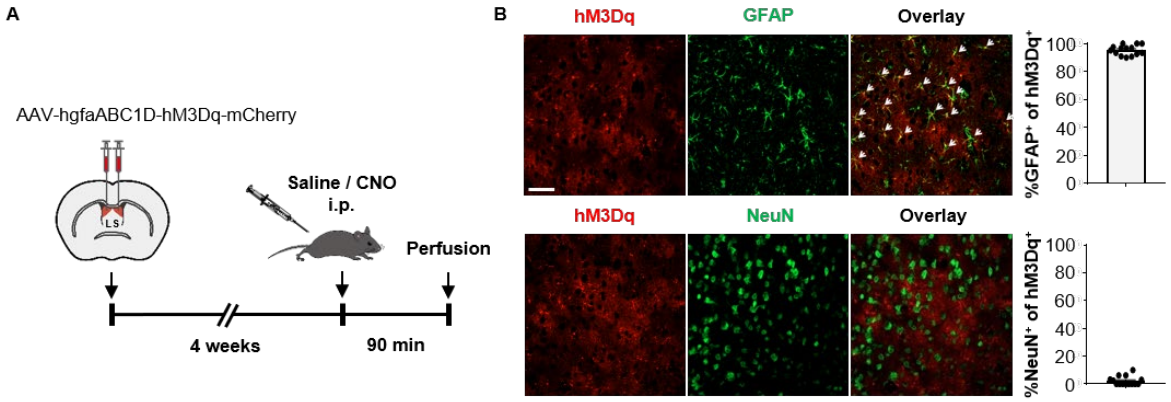
A
AAV-hgfaABC1D-hM3Dq-mCherry
LS
Saline / CNO
i.p.
Perfusion
4 weeks
90 min
B
hM3Dq
GFAP
Overlay
%GFAP+ of hM3Dq+
100
80
60
40
20
0
hM3Dq
NeuN
Overlay
%NeuN+ of hM3Dq+
100
80
60
40
20
0

Figure 3. hM3Dq is specifically expressed in LS astrocytes by hgfaABC1D promoter.

(A) Schematic diagram of virus injection in the LS and experimental timeline. (B) (up) Representative immunohistochemistry images of hM3Dq (red) and GFAP (green) expression in the LS and Quantification of GFAP-positive cells out of hM3Dq-positive cells (n=15 slices from 5 mice, 474 cells). Colocalized hM3Dq and GFAP indicated by white arrows. Scale bars: 50 μm. (down) Representative immunohistochemistry images of hM3Dq (red) and NeuN (green) expression in the LS and Quantification of NeuN-positive cells out of hM3Dq-positive cells (n=15 slices from 5 mice, 474 cells). No colocalization with NeuN. Data are represented as mean ± S.E.M.

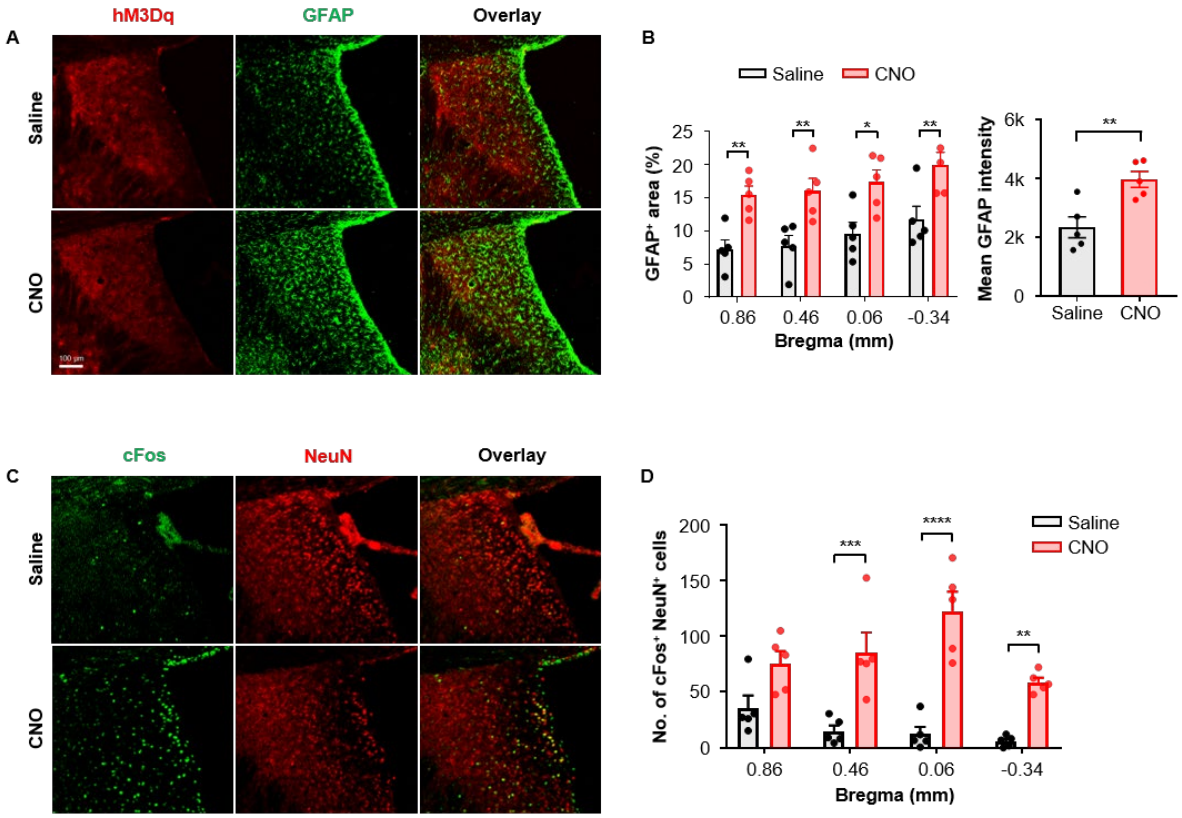
A
hM3Dq
GFAP
Overlay
Saline
CNO
B
Saline
CNO
GFAP⁺ area (%)
25
20
15
10
5
0
**
**
*
**
0.86
0.46
0.06
-0.34
Bregma (mm)
Mean GFAP intensity
6k
4k
2k
0
**
Saline
CNO
C
cFos
NeuN
Overlay
Saline
CNO
D
No. of cFos⁺ NeuN⁺ cells
200
150
100
50
0
***
****
**
Saline
CNO
0.86
0.46
0.06
-0.34
Bregma (mm)

Figure 4. Chemogenetic Gq activation of LS astrocytes can induce molecular changes in both neurons and astrocytes.

(A) Representative immunohistochemistry images of hM3Dq (red) and GFAP (green) expression in the LS from mice treated with saline (up) or CNO (down). Scale bars: 100 μm. (B) (left) Quantification of GFAP-positive area in the LS from mice treated with saline or CNO (Two-way ANOVA with Bonferroni test, p=0.0087 (0.86), p=0.0078 (0.46), p=0.0136 (0.06), p=0.0081 (-0.34); saline n=5, CNO n=5). (right) Quantification of average GFAP intensity in the LS from mice treated with saline or CNO (Unpaired t test, p=0.0068; saline n=5, CNO n=5). (C) Representative immunohistochemistry images of cFos (green) colocalization with NeuN (green) in the LS from hM3Dq-expressing mice treated with saline (up) or CNO (down). (D) The number of cFos-positive neurons in the LS from hM3Dq-expressing mice treated with saline or CNO (Two-way ANOVA with Bonferroni test, p=0.0596 (0.86), p=0.0003 (0.46), p<0.0001 (0.06), p=0.0072 (-0.34); saline n=5, CNO n=5). Data are represented as mean ± S.E.M. *p < 0.05, **p < 0.01, ***p < 0.001, ****p < 0.0001; n.s., not significant.

3.3 Gq pathway activation in LS astrocytes is not sufficient to induce behavioral changes in stress-naïve mice.

Next, we investigated whether astrocytic activation itself can induce behavioral phenotypes seen in the CSDS model in naïve mice. To test this, the viral vectors expressing hM3Dq or EGFP in astrocytes (AAV5-hgfaABC1D-hM3Dq-mCherry or AAV5-hgfaABC1D-EGFP) were injected into the LS. After four weeks of viral incubation, the mice were i.p. injected with CNO (3 mg/kg) 30 min before behavior assays, and depression- and anxiety-related behaviors were assessed using SI, FS, OF, and EPM tests (Fig. 5A). However, there were no differences in behaviors between hM3Dq and EGFP-expressing mice (Fig. 5B, C, D, E). Additionally, we also examined whether chronic activation of LS astrocytes for 10 days, similar to the CSDS period, could affect behaviors (Fig. 5F). Like acute activation, chronic activation of LS astrocytes also did not make alterations in the assessed behaviors (Fig. 5G, H, I, J). Thus, neither acute nor chronic activation of LS astrocytes is sufficient to affect behaviors in stress-naïve mice.

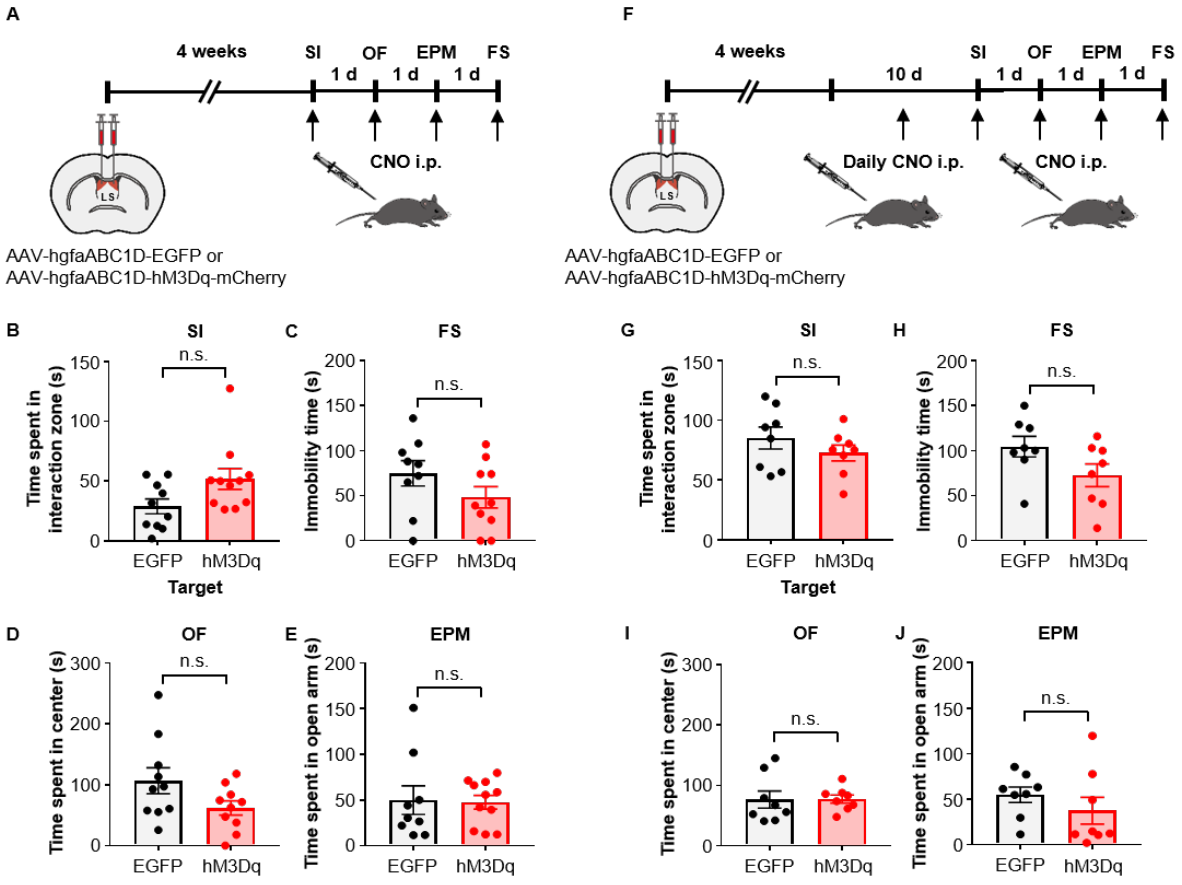
A
4 weeks
SI
OF
EPM
FS
1 d
1 d
1 d
CNO i.p.
LS
AAV-hgfaABC1D-EGFP or
AAV-hgfaABC1D-hM3Dq-mCherry
F
4 weeks
10 d
SI
OF
EPM
FS
1 d
1 d
1 d
Daily CNO i.p.
CNO i.p.
LS
AAV-hgfaABC1D-EGFP or
AAV-hgfaABC1D-hM3Dq-mCherry
B
SI
Time spent in interaction zone (s)
n.s.
EGFP
hM3Dq
Target
C
FS
Immobility time (s)
n.s.
EGFP
hM3Dq
G
SI
Time spent in interaction zone (s)
n.s.
EGFP
hM3Dq
Target
H
FS
Immobility time (s)
n.s.
EGFP
hM3Dq
D
OF
Time spent in center (s)
n.s.
EGFP
hM3Dq
E
EPM
Time spent in open arm (s)
n.s.
EGFP
hM3Dq
I
OF
Time spent in center (s)
n.s.
EGFP
hM3Dq
J
EPM
Time spent in open arm (s)
n.s.
EGFP
hM3Dq

Figure 5. Acute or chronic Gq activation of LS astrocytes is insufficient for evoking depressive- and anxiety-like behaviors in stress-naïve mice.

(A) Schematic diagram of virus injection in the LS and experimental timeline of acute Gq activation. (B) Time spent in the interaction zone during the target session of SI test (Mann-Whitney test, p=0.0845; control n=10, defeated n=11). (C) Immobility time in FS test (Mann-Whitney test, p=0.2331; control n=9, defeated n=10). (D) Time spent in the center zone of OF test (Mann-Whitney test, p=0.1655; control n=10, defeated n=10). (E) Time spent in the open arms of EPM test (Mann-Whitney test, p=0.5516; control n=9, defeated n=11). (F) Schematic diagram of virus injection in the LS and experimental timeline of chronic Gq activation. (G) Time spent in the interaction zone during the target session of SI test (Mann-Whitney test, p=0.3823; control n=8, defeated n=8). (H) Immobility time in FS test (Mann-Whitney test, p=0.1086; control n=8, defeated n=8). (I) Time spent in the center zone of OF test (Mann-Whitney test, p=0.4418; control n=8, defeated n=8). (J) Time spent in the open arms of EPM test (Mann-Whitney test, p=0.2345; control n=8, defeated n=8). Data are represented as mean ± S.E.M. n.s., not significant.

3.4 Activation of LS astrocytes promotes stress-evoked behaviors under subthreshold social defeat stress.

Since activation of LS astrocytes alone was not sufficient to induce behavioral changes in stress-naïve mice, we aimed to examine whether increasing astrocytic activity in the LS through Gq activation could promote stress-evoked behaviors under subthreshold stress. To this end, we adopted subthreshold social defeat stress (SSDS) paradigm which has been used to investigate mechanisms mediating stress susceptibility (Chaudhury et al., 2012, Shen et al., 2019). In this paradigm, mice receive physical attack for 10 min followed by 10 min sensory contact and 5 min of rest in home cage, which is repeated two times (Fig. 6A). We injected an AAV expressing hgfaABC1D promoter-driven hM3Dq or mCherry (AAV5-hgfaABC1D-hM3Dq-mCherry or AAV5-hgfaABC1D-mCherry) into the LS and stimulated astrocytic activation in this region during the SSDS paradigm four weeks after surgery. Mice were then subjected to behavioral assays after CNO (3 mg/kg) injection (Fig. 6A). Under SSDS paradigm, mCherry-expressing mice did not exhibit social avoidance in the SI test (Fig. 6B). Notably, the hM3Dq group dramatically spent less time in the interaction zone during the target session (Fig. 6B) and showed increased immobility time in the FS test (Fig. 6C) than mCherry group. Moreover, astrocyte activation with SSDS increased anxiety-like behaviors in the OF and the EPM tests (Fig. 6D, E). To specifically determine the causal effect of astrocytic activation in modulating behaviors, we activated LS astrocytes only during SSDS and measured behaviors without CNO injection (Fig. 6F). Mice treated with CNO only in the SSDS paradigm showed no behavioral changes in all tests performed (Fig. 6G, H, I, J). These results imply that continuous Gq activation of LS astrocytes promotes stress-evoked depressive- and anxiety-like behaviors following SSDS.

To further examine the effect of SSDS on the LS when astrocytic Gq pathway is activated, we conducted a cFos induction test as the expression of cFos can serve as an indicator of cellular responses induced by psychomotor stimulants. First, mice were bilaterally injected with AAV5-hgfaABC1D-hM3Dq-mCherry or AAV5-hgfaABC1D-mCherry to the LS. Four weeks later, CNO (3 mg/kg) was administered intraperitoneally, and brains were collected 120 min later. For 120 min, the control group stayed in their home cage, whereas the SSDS group underwent SSDS for 50 min, 20 min after CNO injection, and rested in home cage for the remaining 50 min (Fig. 7A). The staining for cFos revealed that SSDS combined with astrocytic Gq activation dramatically increased cFos expression levels in the LS, compared to the effect of SSDS alone or astrocytic Gq activation alone (Fig. 7B, C). Additionally, co-staining with the neuronal marker NeuN showed that SSDS affected only neuronal activity, while SSDS under Gq activation in LS astrocytes induced increased activity not only in neurons but also in astrocytes (Fig. 7D, E, F, G). Therefore, subthreshold stress can sensitize LS neurons, and this effect can be augmented by activating astrocytic Gq pathway in the LS.

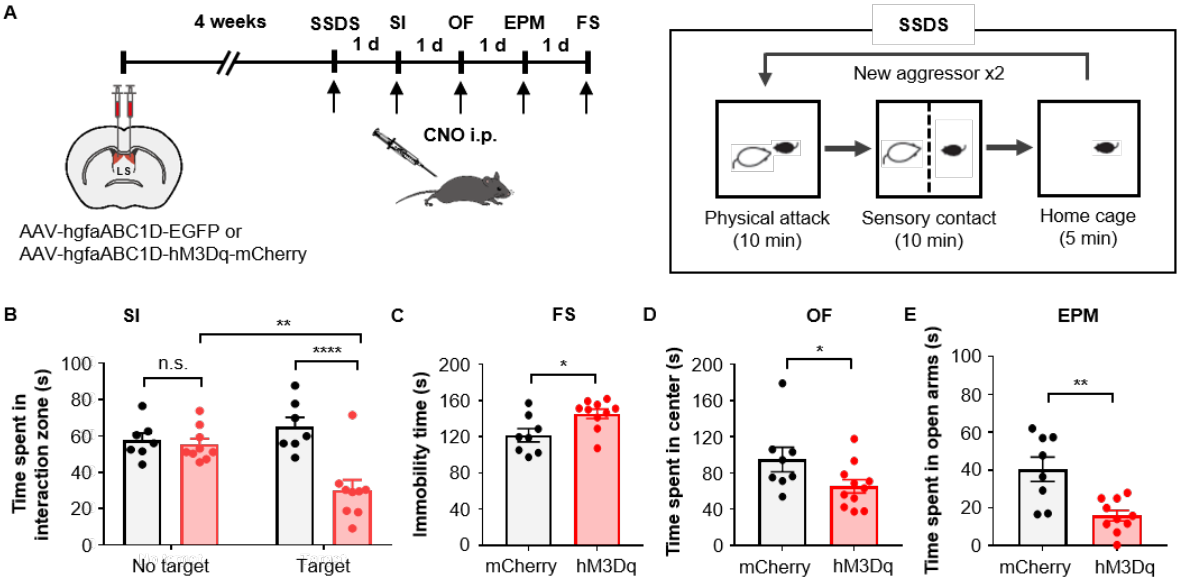
A
4 weeks
SSDS
SI
OF
EPM
FS
1 d
1 d
1 d
1 d
CNO i.p.
LS
AAV-hgfaABC1D-EGFP or
AAV-hgfaABC1D-hM3Dq-mCherry
SSDS
New aggressor x2
Physical attack
(10 min)
Sensory contact
(10 min)
Home cage
(5 min)
B
SI
Time spent in interaction zone (s)
n.s.
**
****
No target
Target
C
FS
Immobility time (s)
*
mCherry
hM3Dq
D
OF
Time spent in center (s)
*
mCherry
hM3Dq
E
EPM
Time spent in open arms (s)
**
mCherry
hM3Dq

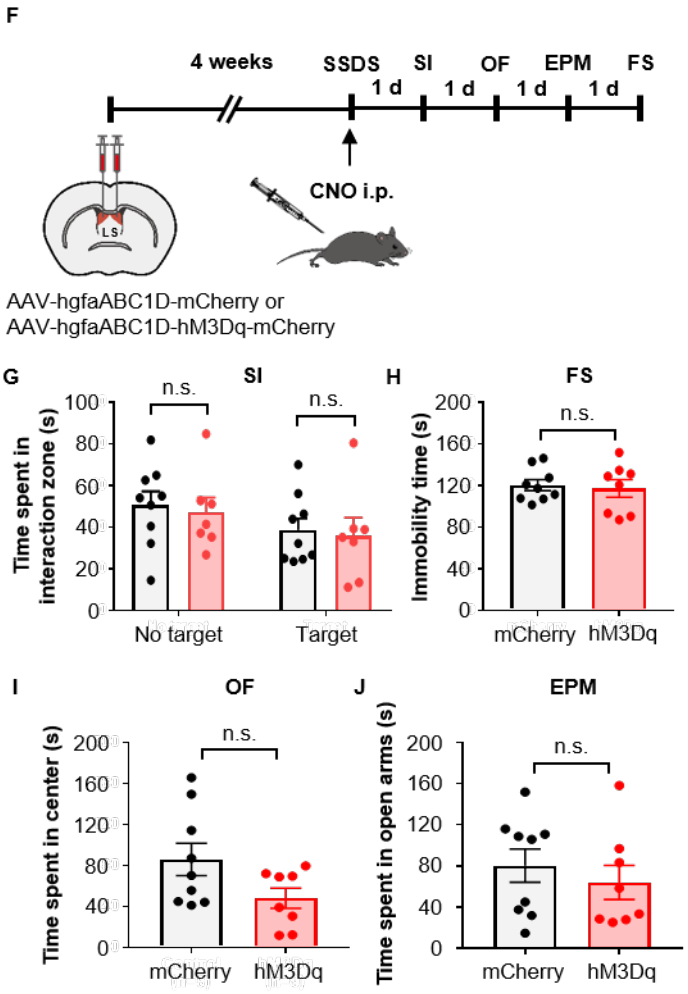
F
4 weeks
SSDS
1 d
SI
1 d
OF
1 d
EPM
1 d
FS
CNO i.p.
LS
AAV-hgfaABC1D-mCherry or
AAV-hgfaABC1D-hM3Dq-mCherry
G
SI
Time spent in interaction zone (s)
n.s.
n.s.
No target
Target
H
FS
Immobility time (s)
n.s.
mCherry
hM3Dq
I
OF
Time spent in center (s)
n.s.
mCherry
hM3Dq
J
EPM
Time spent in open arms (s)
n.s.
mCherry
hM3Dq

Figure 6. Gq activation of LS astrocytes can elicit depressive- and anxiety-like behaviors in mice exposed to subthreshold social defeat stress.

(A) Schematic diagram of virus injection in the LS and experimental timeline of subthreshold social defeat stress. (B) Time spent in the interaction zone during the target session of SI test (Two-way ANOVA with Bonferroni test, no target: $p>0.9999$ or target: $p<0.0001$, mCherry: $p>0.9999$ or hM3Dq: $p=0.0024$; mCherry n=7, hM3Dq n=9). (C) Immobility time in FS test (Mann-Whitney test, $p=0.0205$; mCherry n=8, hM3Dq n=10). (D) Time spent in the center zone of OF test (Mann-Whitney test, $p=0.0409$; mCherry n=8, hM3Dq n=11). (E) Time spent in the open arms of EPM test (Mann-Whitney test, $p=0.0031$; mCherry n=8, hM3Dq n=10). (F) Schematic diagram of virus injection in the LS and experimental timeline. (G) Time spent in the interaction zone during the target session of SI test (Two-way ANOVA with Bonferroni test, no target: $p>0.9999$ or target: $p>0.9999$, mCherry: $p>0.9999$ or hM3Dq: $p>0.9999$; mCherry n=9, hM3Dq n=7). (H) Immobility time in FS test (Mann-Whitney test, $p=0.9626$; mCherry n=9, hM3Dq n=8). (I) Time spent in the center zone of OF test (Mann-Whitney test, $p=0.0927$; mCherry n=9, hM3Dq n=8). (J) Time spent in the open arms of EPM test (Mann-Whitney test, $p=0.3282$; mCherry n=8, hM3Dq n=8). Data are represented as mean ± S.E.M. $*p < 0.05$, $**p < 0.01$, $***p < 0.001$, $****p < 0.0001$; n.s., not significant.

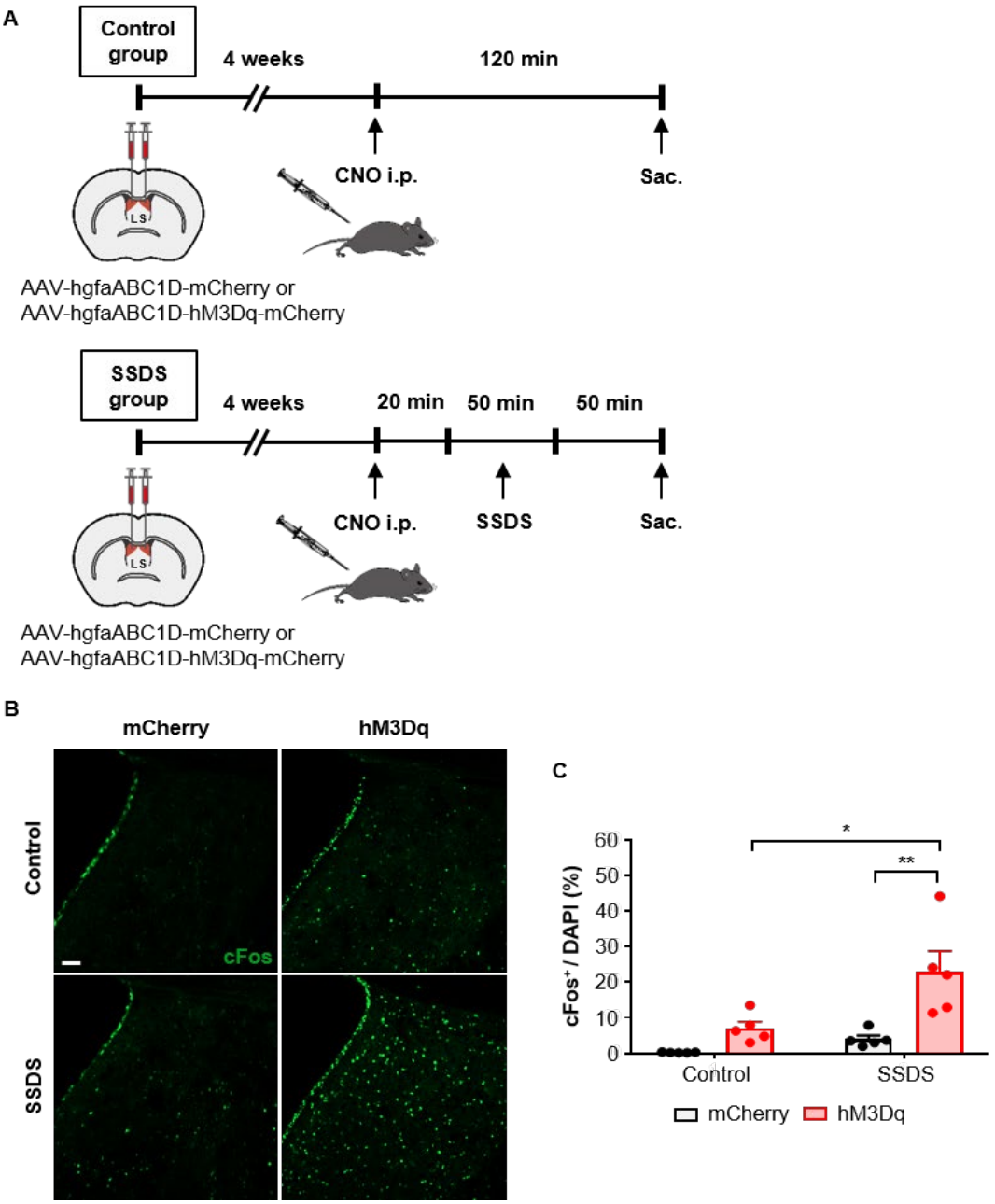
A
Control group
4 weeks
120 min
CNO i.p.
Sac.
LS
AAV-hgfaABC1D-mCherry or
AAV-hgfaABC1D-hM3Dq-mCherry
SSDS group
4 weeks
20 min
50 min
50 min
CNO i.p.
SSDS
Sac.
LS
AAV-hgfaABC1D-mCherry or
AAV-hgfaABC1D-hM3Dq-mCherry
B
mCherry
hM3Dq
Control
SSDS
cFos
C
cFos+ / DAPI (%)
60
50
40
30
20
10
0
*
**
Control
SSDS
mCherry
hM3Dq

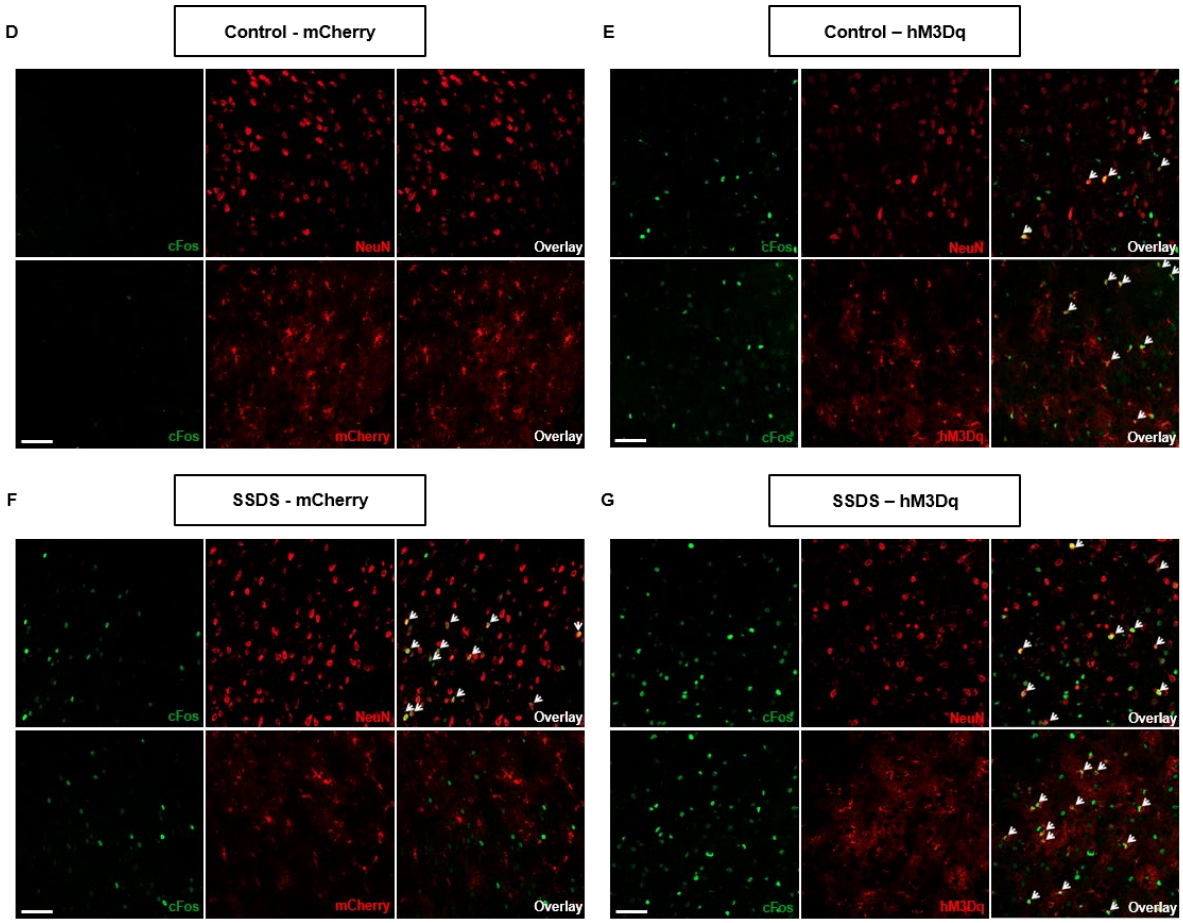
D
Control - mCherry
E
Control – hM3Dq
cFos
NeuN
Overlay
cFos
mCherry
Overlay
cFos
NeuN
Overlay
cFos
hM3Dq
Overlay
F
SSDS - mCherry
G
SSDS – hM3Dq
cFos
NeuN
Overlay
cFos
mCherry
Overlay
cFos
NeuN
Overlay
cFos
hM3Dq
Overlay

Figure 7. Gq activation of LS astrocytes can affect cell activity in the LS when combined with SSDS.

(A) Schematic diagram of virus injection in the LS and experimental timeline of cFos induction test in control group (up) and SSDS group (down). (B) Representative confocal images of cFos expression in the LS from mCherry- or hM3Dq-expressing mice exposed to SSDS or not. Scale bars: 50 μm. (C) Quantification of cFos-positive cells out of DAPI-stained cells (Two-way ANOVA with Bonferroni test, control: $p=0.8201$ or SSDS: $p=0.0033$, mCherry: $p>0.9999$ or hM3Dq: $p=0.0145$; $n=5$ for all groups). (D) (up) Representative immunohistochemistry images of cFos (green) colocalization with NeuN (Red) in the LS from mCherry-expressing mice. (down) Representative immunohistochemistry images of cFos (green) colocalization with mCherry (Red) in the LS from mCherry-expressing mice. Scale bars: 50 μm. (E) (up) Representative immunohistochemistry images of cFos (green) colocalization with NeuN (Red) in the LS from hM3Dq-expressing mice. Colocalized cFos and NeuN indicated by white arrows. (down) Representative immunohistochemistry images of cFos (green) colocalization with hM3Dq (Red) in the LS from hM3Dq-expressing mice. Colocalized cFos and hM3Dq indicated by white arrows. Scale bars: 50 μm. (F) (up) Representative immunohistochemistry images of cFos (green) colocalization with NeuN (Red) in the LS from mCherry-expressing mice exposed to SSDS. Colocalized cFos and NeuN indicated by white arrows. (down) Representative immunohistochemistry images of cFos (green) colocalization with mCherry (Red) in the LS from mCherry-expressing mice exposed to SSDS. No colocalization with mCherry. Scale bars: 50 μm. (G) (up) Representative immunohistochemistry images of cFos (green) colocalization with NeuN (Red) in the LS from hM3Dq-expressing mice exposed to SSDS. Colocalized cFos and NeuN indicated by white arrows. (down)

Representative immunohistochemistry images of cFos (green) colocalization with hM3Dq (Red) in the LS from hM3Dq-expressing mice exposed to SSDS. Colocalized cFos and hM3Dq indicated by white arrows. Scale bars: 50 μm. Data are represented as mean ± S.E.M. *$p < 0.05$, **$p < 0.01$.

3.5 Calcium signaling in astrocytes is required for neural activity induced by social defeat stress in the LS.

If increasing calcium signaling in LS astrocytes by Gq pathway activation can promote stress-evoked behaviors under subthreshold stress, we hypothesized that artificially decreasing calcium signaling in LS astrocytes could contribute to those behaviors oppositely. Previous studies have shown that human plasma membrane Ca^{2+} ATPase isoform type 2 with the w/b splice variant (hPMCA2w/b) significantly reduced calcium signals by extruding cytosolic calcium into extracellular space and was sufficient to induce behavioral changes in mice when expressed in astrocytes (Yu et al., 2018, Erickson et al., 2020). We first delivered viral vectors expressing hPMCA2w/b or mCherry with an astrocyte-specific hgfaABC1D promoter (AAV5-hgfaABC1D-mCherry-hPMCA2w/b or AAV5-hgfaABC1D-mCherry) in the LS (Fig. 8A). Histological analysis showed that more than 90% of mCherry-expressing cells and hPMCA2w/b-expressing cells were colocalized with an astrocyte marker GFAP and rarely merged with a neuronal marker NeuN (Fig. 8B, C).

Next, we aimed to demonstrate whether hPMCA2w/b expression in LS astrocytes could suppress astrocytic activity effectively. As acute social defeat stress (SDS) has been reported to induce an increase of cell activity indicated by altered cFos levels in stress-related brain regions including the LS (Matsuda et al., 1996, Numa et al., 2019), we examined if decreasing astrocytic calcium signaling in the LS could prevent the activity increase induced by SDS. Mice expressing hPMCA2w/b or mCherry in LS astrocytes were exposed to 10 min of social defeat stress and then had sensory contact time with the aggressor for 90 min. Brains were collected immediately after sensory contact is over and stained for the immediate early gene cFos in the LS and other depression-related

brain regions (Fig. 8A). For control groups, the mice expressing hPMCA2w/b or mCherry were remained in their home cages for 100 min and perfused in the same way. As previously reported, acute SDS significantly increased cFos expression in the LS when comparing the defeated mCherry group with the control mCherry group (Fig. 9A, B). Most cFos-positive cells were found to be overlapped with a neuronal marker NeuN (Fig. 9C). Importantly, inhibiting astrocytic calcium signaling by hPMCA2w/b significantly reduced the number of cFos-positive cells in the LS (Fig. 9A, B). This reduction was caused by astrocyte-specific expression of hPMCA2w/b in the LS since there was no alteration of cFos expression in other brain regions, such as ventral LS (vLS), cingulate cortex (Cg), infralimbic cortex (IL), and prelimbic cortex (PrL) (Fig. 9D). Taken together, these results suggest that reducing astrocytic calcium signals can block SDS-induced neuronal activity in the LS.

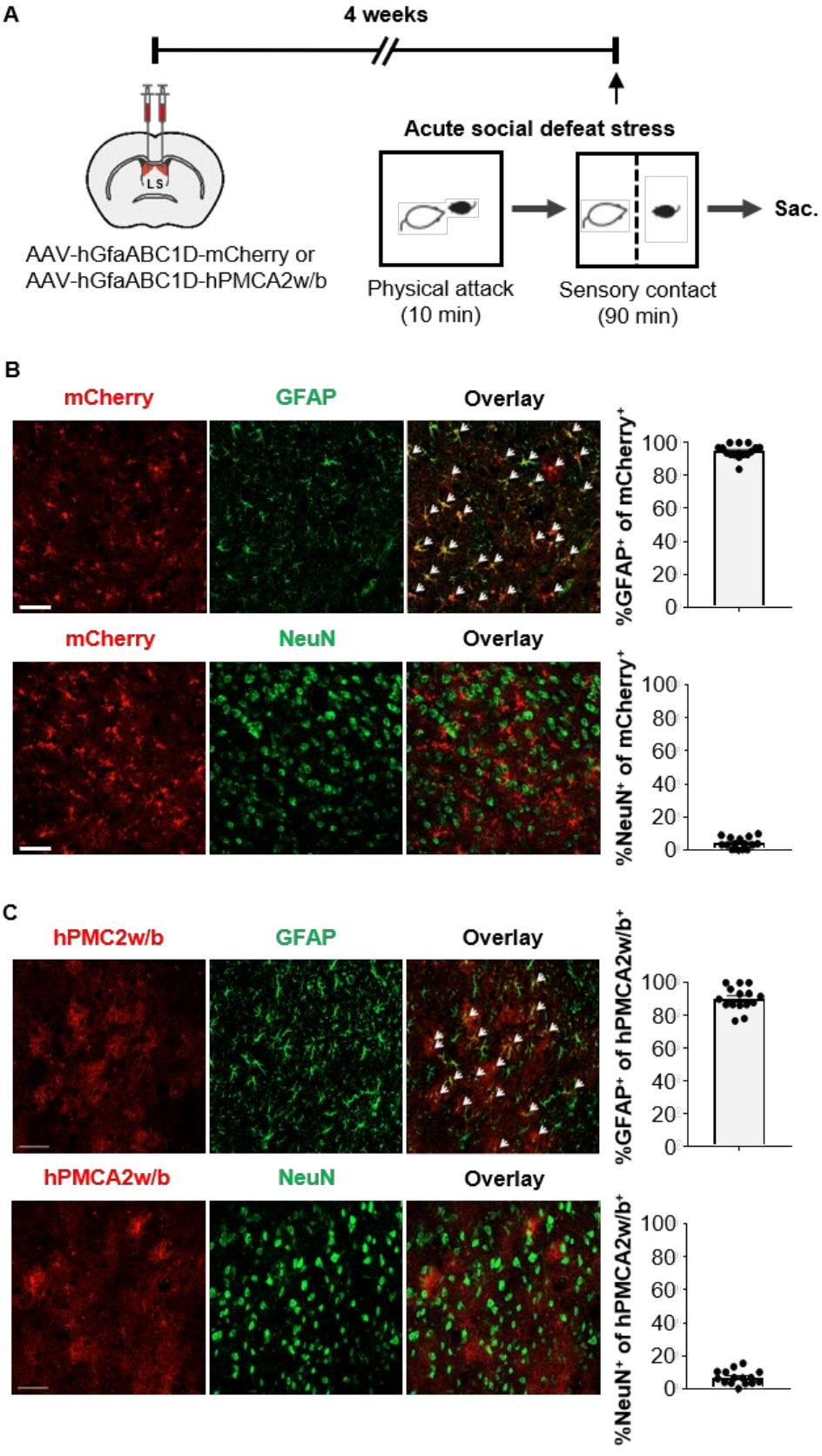
A
4 weeks
LS
AAV-hGfaABC1D-mCherry or
AAV-hGfaABC1D-hPMCA2w/b
Acute social defeat stress
Physical attack
(10 min)
Sensory contact
(90 min)
Sac.
B
mCherry
GFAP
Overlay
%GFAP+ of mCherry+
mCherry
NeuN
Overlay
%NeuN+ of mCherry+
C
hPMC2w/b
GFAP
Overlay
%GFAP+ of hPMCA2w/b+
hPMCA2w/b
NeuN
Overlay
%NeuN+ of hPMCA2w/b+
0
20
40
60
80
100

Figure 8. hPMCA2w/b is specifically expressed in LS astrocytes by hgfaABC1D promoter.

(A) Schematic diagram of virus injection in the LS and experimental timeline of acute social defeat stress. (B) (up) Representative immunohistochemistry images of mCherry (red) and GFAP (green) expression in the LS and Quantification of GFAP-positive cells out of mCherry-positive cells (n=15 slices from 5 mice, 466 cells). Colocalized mCherry and GFAP indicated by white arrows. Scale bars: 50 μm. (down) Representative immunohistochemistry images of mCherry (red) and NeuN (green) expression in the LS and Quantification of NeuN-positive cells out of mCherry-positive cells (n=15 slices from 5 mice, 466 cells). No colocalization with NeuN. (C) (up) Representative immunohistochemistry images of hPMCA2w/b (red) and GFAP (green) expression in the LS and Quantification of GFAP-positive cells out of hPMCA2w/b-positive cells (n=15 slices from 5 mice, 443 cells). Colocalized hPMCA2w/b and GFAP indicated by white arrows. Scale bars: 50 μm. (down) Representative immunohistochemistry images of hPMCA2w/b (red) and NeuN (green) expression in the LS and Quantification of NeuN-positive cells out of hPMCA2w/b-positive cells (n=15 slices from 5 mice, 443 cells). No colocalization with NeuN. Data are represented as mean ± S.E.M.

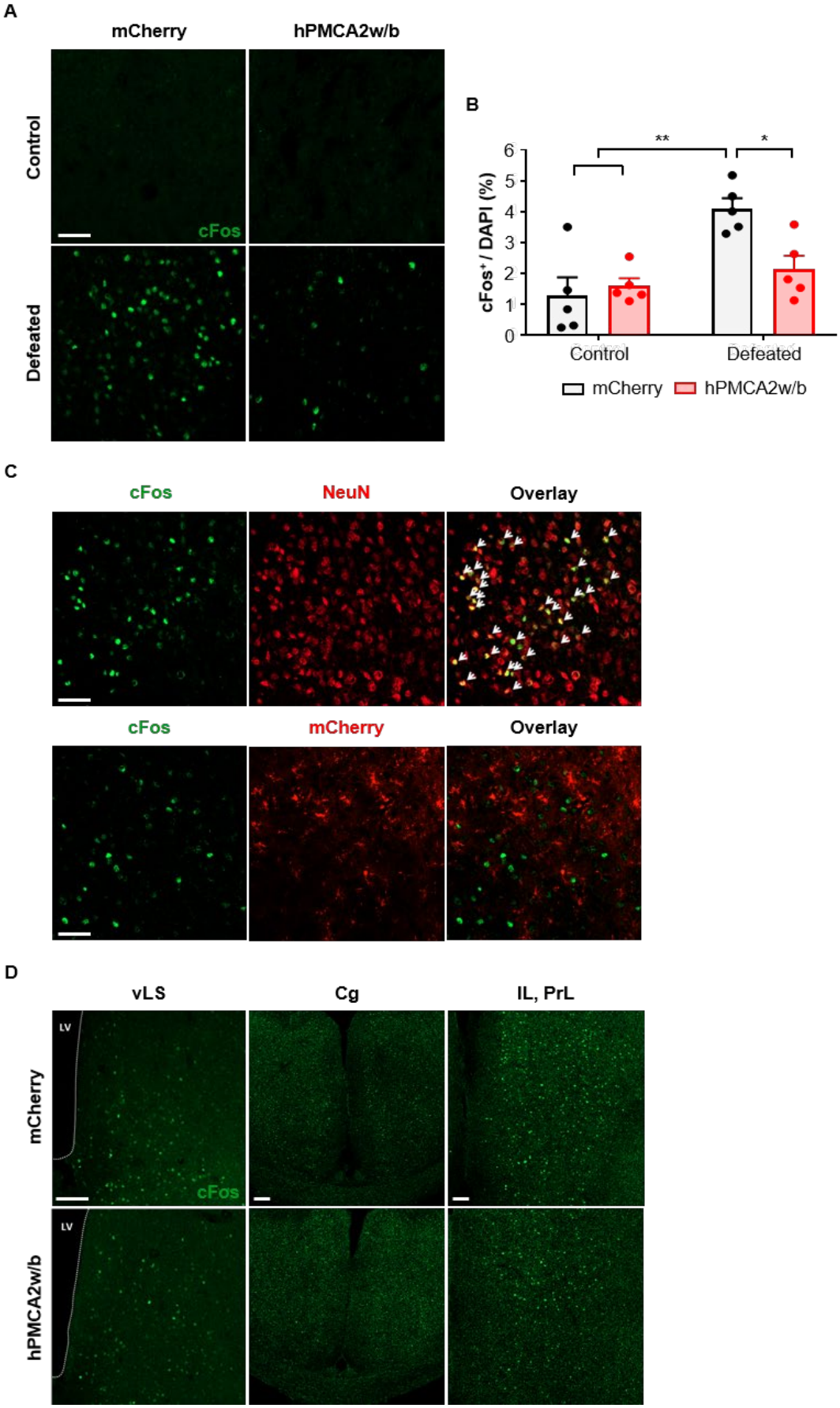
A
mCherry
hPMCA2w/b
Control
Defeated
cFos
B
cFos+ / DAPI (%)
0
1
2
3
4
5
6
**
*
Control
Defeated
mCherry
hPMCA2w/b
C
cFos
NeuN
Overlay
cFos
mCherry
Overlay
D
vLS
Cg
IL, PrL
mCherry
hPMCA2w/b
LV
LV
cFos

Figure 9. Reducing calcium signaling of astrocytes in the LS can block neuronal activity evoked by acute social defeat stress.

(A) Representative confocal images of cFos expression in the LS from mCherry- or hPMCA2w/b-expressing mice exposed to acute social defeat stress or not. Scale bars: 50 μm. (B) Quantification of cFos-positive cells out of DAPI-stained cells (Two-way ANOVA with Bonferroni test, control: $p>0.9999$ or defeated: $p=0.0307$, mCherry: $p=0.0015$ or hPMCA2w/b: $p>0.9999$; $n=5$ for all groups). (C) (up) Representative immunohistochemistry images of cFos (green) colocalization with NeuN (Red) in the LS from defeated mCherry-expressing mice. Colocalized cFos and NeuN indicated by white arrows. Scale bars: 50 μm. (down) Representative immunohistochemistry images of cFos (green) colocalization with mCherry (Red) in the LS from defeated mCherry-expressing mice. No colocalization with mCherry. (D) Representative confocal images of cFos expression in the vLS, Cg, IL, and PrL from mCherry- or hPMCA2w/b-expressing mice exposed to acute social defeat stress. Scale bars: 50 μm. Data are represented as mean ± S.E.M. $*p < 0.05$, $**p < 0.01$.

3.6 LS astrocytic calcium signaling is necessary for depressive-like behaviors induced by CSDS.

We next addressed whether CSDS-induced depressive- and anxiety-like behaviors could be reversed by suppressing calcium signaling of LS astrocytes. Four weeks after viral injection, depression- and anxiety-related behaviors were measured in both hPMCA2w/b- and mCherry-expressing mice after exposure to CSDS or not (Fig. 10A). CSDS-exposed mice receiving the mCherry virus exhibited typical depressive-like phenotypes with increased social avoidance and immobility time in FS (Fig. 10B, C). Interestingly, defeated mice expressing hPMCA2w/b showed an increase in the social interaction, as well as an improvement in the FS test compared to defeated mCherry-expressing mice (Fig. 10B, C). However, CSDS-induced anxiety-related behaviors were not affected by hPMCA2w/b expression in LS astrocytes (Fig. 10D, E). In the non-defeated control group, both hPMCA2w/b- and mCherry-expressing mice exhibited similar behaviors in SI, FS, OF, and EPM tests (Fig. 10B, C, D, E). These data indicate that calcium signaling in LS astrocytes is necessary for depression-related behaviors evoked by CSDS, but not for anxiety-like behaviors.

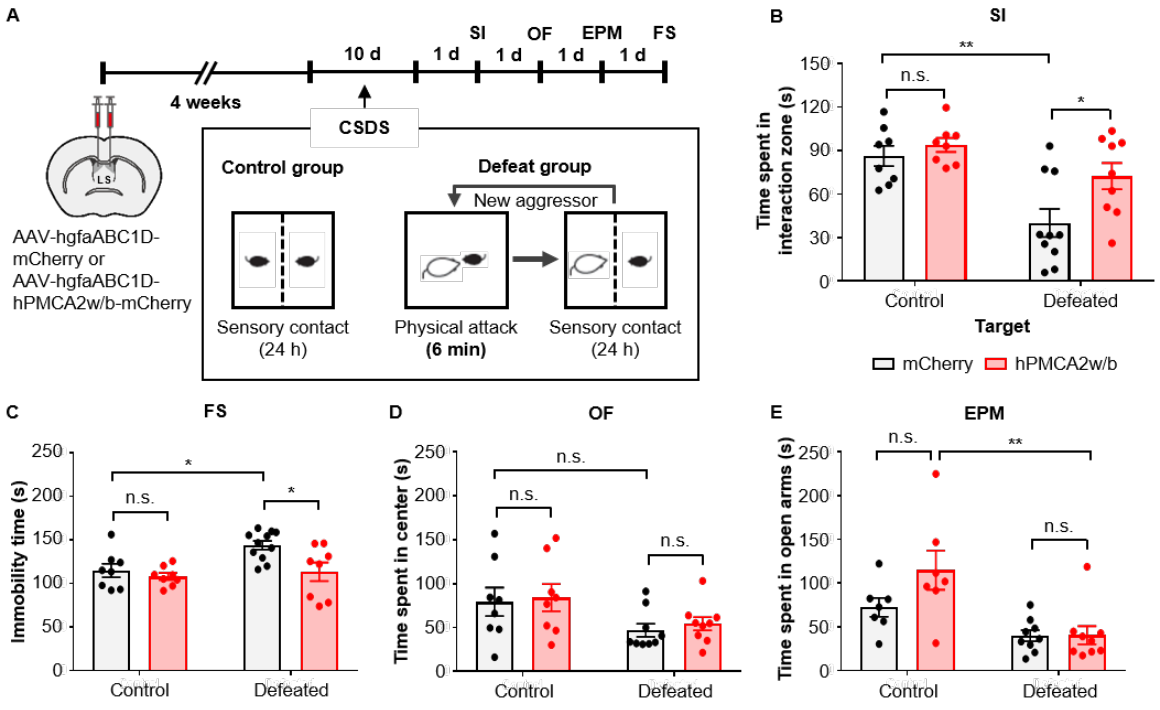
A
SI
OF
EPM
FS
10 d
1 d
1 d
1 d
1 d
4 weeks
CSDS
LS
Control group
Defeat group
New aggressor
AAV-hgfaABC1D-mCherry or AAV-hgfaABC1D-hPMCA2w/b-mCherry
Sensory contact (24 h)
Physical attack (6 min)
Sensory contact (24 h)
B
SI
Time spent in interaction zone (s)
n.s.
**
*
Control
Defeated
Target
mCherry
hPMCA2w/b
C
FS
Immobility time (s)
n.s.
*
*
Control
Defeated
D
OF
Time spent in center (s)
n.s.
n.s.
n.s.
Control
Defeated
E
EPM
Time spent in open arms (s)
n.s.
**
n.s.
Control
Defeated

Figure 10. Astrocytes in the LS are necessary for CDSD-elicited depressive-like behaviors, but not anxiety-like behaviors.

(A) Schematic diagram of virus injection in the LS and experimental timeline. (B) Time spent in the interaction zone during the target session of SI test (Two-way ANOVA with Bonferroni test, control: $p>0.9999$ or defeated: $p=0.0431$, mCherry: $p=0.0023$ or hPMCA2w/b: $p=0.4734$; control mCherry n=8, control hPMCA2w/b n=8, defeated mCherry n=10, defeated hPMCA2w/b n=9). (C) Immobility time in FS test (Two-way ANOVA with Bonferroni test, control: $p>0.9999$ or defeated: $p=0.0207$, mCherry: $p=0.0309$ or hPMCA2w/b: $p>0.9999$; control mCherry n=8, control hPMCA2w/b n=8, defeated mCherry n=11, defeated hPMCA2w/b n=9). (D) Time spent in the center zone of OF test (Two-way ANOVA with Bonferroni test, control: $p>0.9999$ or defeated: $p>0.9999$, mCherry: $p=0.3862$ or hPMCA2w/b: $p=0.5225$; control mCherry n=8, control hPMCA2w/b n=8, defeated mCherry n=9, defeated hPMCA2w/b n=9). (E) Time spent in the open arms of EPM test (Two-way ANOVA with Bonferroni test, control: $p=0.2158$ or defeated: $p>0.9999$, mCherry: $p=0.5143$ or hPMCA2w/b: $p=0.0020$; control mCherry n=7, control hPMCA2w/b n=7, defeated mCherry n=9, defeated hPMCA2w/b n=9). Data are represented as mean ± S.E.M. $*p < 0.05$, $**p < 0.01$; n.s., not significant.

IV. DISCUSSION

In the present study, we provide several lines of evidence supporting the contribution of LS astrocytes in regulating depressive- and anxiety-like behaviors evoked by social defeat stress. After CSDS, astrocytes in the LS were activated in a delayed manner. We found that features altered in LS astrocytes by CSDS were related to reactive astrocytes seen in many neurological disorders, such as neurotrauma, ischemic stroke, and neurodegenerative disease. Reactive astrocytes show upregulation of GFAP, widely used as a marker of reactive astrocytes, and hypertrophy on a morphological level (Hol and Pekny, 2015; Shigetomi et al., 2019). Our results confirmed that GFAP expression and cell complexity were increased in LS astrocytes of defeated mice. However, the underlying molecular mechanisms of delayed changes of LS astrocytes by CSDS are still elusive.

Since reactive astrocytes are known to release different gliotransmitters compared to non-reactive astrocytes, they can affect nearby neuronal activity, and even neural circuits and behaviors. For example, the brain ATP level was decreased in the mice that were susceptible to CSDS, and ATP from astrocytes is sufficient and necessary for depressive-like behaviors (Cao et al., 2013). In addition, astrocytic potassium channel Kir4.1 and extracellular glutamate uptake in the lateral habenula (LHb) play critical roles in modulating the degree of LHb neuronal bursting and depression-like symptoms (Cui et al., 2014; Cui et al., 2018). Lastly, the reduction of multiple endocrine neoplasia type 1 (Men1) in astrocytes enhanced inflammatory responses (NF-κB activation and IL-1β production) leading to depressive-like behaviors in mice (Leng et al., 2018). These studies suggest that astrocytes have various potential roles in depressive disorder, but studies on the role of astrocytes in depression have been conducted in only a few brain areas despite the heterogeneity of region-specific astrocytic

functions.

In this study, we focused on the lateral septum (LS), a brain region connected with many other areas related to depression including the hippocampus, medial prefrontal cortex (mPFC), ventral tegmental area (VTA), and nucleus accumbens (NAc) (Sheehan et al., 2004). The LS has previously been implicated in the regulation of mood and stress responses (Anthony et al., 2014; Parfitt et al., 2017; Sheehan et al., 2004). For example, oxytocin receptor-expressing LS neurons reduced a fear-conditioned response following social defeat stress and blocking GLP-1R signaling in the LS attenuated stress-induced suppression of feeding (Guzman et al., 2013; Terrill et al., 2018). In addition, somatostatin-expressing interneurons in the dorsolateral LS respond to foot-shock stress and regulate conditional fear responses, indicating a role of LS neurons in fear responses to external threats (Besnard et al., 2019). Importantly, LS neurons are also involved in depressive-like behaviors (Sheehan et al., 2004). Metabolic activity of the LS was correlated with the helplessness behavior induced by foot-shock, and serotonin (5-HT) signaling of the LS modulates depression-like behavior in rats (Ebner et al., 2007, Mirrione et al., 2014, Singewald et al., 2010). Collectively, previous studies suggest that astrocytes in the LS region can be involved in modulating stress-induced depressive- and anxiety-like behaviors.

Based on previous studies shown the ability of Gq-coupled receptor hM3Dq inducing elevation of calcium signaling in astrocytes, we chose to express hM3Dq in LS astrocytes to activate astrocytes (Adamsky et al., 2018; Agulhon et al., 2008; Araque et al., 2014). When calcium signaling is increased by Gq pathway activation in astrocytes, they display an excitable form and play active roles in brain information processing (Agulhon et al., 2008; Guerra-Gomes et al., 2018). Our chemogenetic

manipulation of LS astrocytes demonstrates that DREADD-mediated activation of astrocytic calcium signaling in the LS was not sufficient to alter behavioral responses in stress-naïve mice, even though it increased astrocytic activity and nearby neuronal activity on a cellular level. Since the LS participates in regulating behavioral responses to deal with environmental demands effectively, manipulating LS astrocytes in naïve mice may have no effect on basic behaviors (Sheehan et al., 2004). Notably, this manipulation promoted stress-evoked behaviors including social avoidance, depressive- and anxiety-like behaviors following SSDS. A recent study shows that GABAergic neurons in the LS can modulate depression-related behaviors through neuronal projections to the periaqueductal gray (PAG) (Wang et al., 2021). It has been shown that chemogenetic inhibition of GABAergic neurons in the LS rescues depressive phenotypes of the chronic unpredictable stress (CUS) model. Since we observed that the SSDS paradigm can induce neuronal activity in the LS and chemogenetic activation of LS astrocytes can increase additional neural and astrocytic activity when SSDS is added, further studies can be conducted by regulating neighboring LS neurons which are affected by astrocytic manipulation.

To decrease astrocytic activity in the LS, hPMCA2w/b was used to manipulate calcium signaling in LS astrocytes. In the previous study, hPMCA2w/b was used because it has a high pump rate, lacks cytosolic interaction domains, and effectively reduced ATP-evoked calcium signals over 95% in HEK293 cells (Yu et al., 2018). Our result shows that hPMCA2w/b-mediated inhibition of LS astrocytes blocked neural activity increased by acute SDS and reversed depression-related behaviors after CSDS. However, anxiety-like behaviors were not affected by hPMCA2w/b expression. We assumed that the constitutive function of hPMCA2w/b extruding cytosolic calcium might act differently from

the time-restricted activation of Gq pathway by CNO. In addition, the number of hPMCA2w/b-infected astrocytes or the reduced level of calcium signaling in LS astrocytes might not be sufficient to induce rescued anxiety-like behaviors. This is because the previous study showed that the magnitude of striatal astrocyte calcium signaling attenuation produced by hPMCA2w/b was smaller than that observed with IP3R2 deletion mice. Although hPMCA2w/b did not affect astrocyte properties, it also did not induce striatal fast synaptic transmission (Yu et al., 2018).

Furthermore, the role of the LS in controlling anxiety is inconsistent. Septal lesions, including both medial and lateral parts, caused the “septal rage” phenotype, characterized by dramatically increased defensive responses to nonthreatening stimuli, suggesting an anxiolytic function of the LS (Brady and Nauta, 1955). Likewise, midazolam infusions into the lateral septal nuclei increased open-arm exploration in the elevated plus-maze test, whereas midazolam infusions into the medial septum did not produce an anxiolytic effect (Pesold and Treit, 1996). On the contrary, other studies demonstrated an anxiogenic role of the LS with decreased anxiety-related behaviors when the LS is inactivated. When the selective corticotropin-releasing factor 2 (CRF2) agonist urocortin 2 was infused into the LS, anxiety-related behaviors are increased (Radulovic et al., 1999; Henry, 2006). Even lower doses were sufficient to increase anxiety-related behaviors in the high-stress condition (Henry, 2006). A recent study implied the anxiolytic function of the LS again, by selectively manipulating individual cell populations projecting to the LS (Parfitt et al., 2017). It suggests that anxiety-reducing function was observed in neural projections from the ventral hippocampus to the LS in a bidirectional manner. Therefore, further research about anxiety-like behaviors induced by LS manipulation is needed.

In conclusion, we identified changes in LS astrocytes induced by CSDS and revealed the

contribution of LS astrocytes in regulating stress-evoked behaviors. By manipulating astrocytic calcium signaling in the LS, we demonstrated that activating LS astrocytes enhanced depressive- and anxiety-like behaviors after subthreshold stress and inhibiting LS astrocytes has an antidepressant effect on chronic stress. Although further investigations are needed to elucidate how LS astrocytes are activated by chronic stress and how reactive astrocytes affect neuronal circuits, these findings expand the limited role of LS astrocytes in stress-related behaviors and provide a novel therapeutic target for treating depression.

References

Caspi, A. “Influence of Life Stress on Depression: Moderation by a Polymorphism in the 5-HTT Gene.” *Science*, vol. 301, no. 5631, 2003, pp. 386–389., doi:10.1126/science.1083968.

Bartolomucci, Alessandro, and Rosario Leopardi. “Stress and Depression: Preclinical Research and Clinical Implications.” *PLoS ONE*, vol. 4, no. 1, 2009, doi:10.1371/journal.pone.0004265.

Heim, Christine, and Charles B Nemeroff. “The Role of Childhood Trauma in the Neurobiology of Mood and Anxiety Disorders: Preclinical and Clinical Studies.” *Biological Psychiatry*, vol. 49, no. 12, 2001, pp. 1023–1039., doi:10.1016/s0006-3223(01)01157-x.

Mariotti, Agnese. “The Effects of Chronic Stress on Health: New Insights into the Molecular Mechanisms of Brain–Body Communication.” *Future Science OA*, vol. 1, no. 3, 2015, doi:10.4155/fso.15.21.

Chaijale, Nayla N, et al. “Repeated Social Stress Increases Reward Salience and Impairs Encoding of Prediction by Rat Locus Coeruleus Neurons.” *Neuropsychopharmacology*, vol. 40, no. 2, 2014, pp. 513–523., doi:10.1038/npp.2014.200.

Berton, O. “Essential Role of BDNF in the Mesolimbic Dopamine Pathway in Social Defeat Stress.” *Science*, vol. 311, no. 5762, 2006, pp. 864–868., doi:10.1126/science.1120972.

Golden, Sam A, et al. “A Standardized Protocol for Repeated Social Defeat Stress in Mice.” *Nature Protocols*, vol. 6, no. 8, 2011, pp. 1183–1191., doi:10.1038/nprot.2011.361.

Buwalda, Rixt T., et al. “Aggregation of Azo Dyes with Cationic Amphiphiles at Low Concentrations in Aqueous Solution.” *Langmuir*, vol. 15, no. 4, 1999, pp. 1083–1089., doi:10.1021/la980824i.

Krishnan, Vaishnav, and Eric J. Nestler. “The Molecular Neurobiology of Depression.” *Nature*, vol. 455, no. 7215, 2008, pp. 894–902., doi:10.1038/nature07455.

Kudryavtseva, N.N., et al. “Social Model of Depression in Mice of C57BL/6J Strain.” *Pharmacology Biochem-*

istry and Behavior, vol. 38, no. 2, 1991, pp. 315–320., doi:10.1016/0091-3057(91)90284-9.

Krishnan, Vaishnav, et al. "Molecular Adaptations Underlying Susceptibility and Resistance to Social Defeat in Brain Reward Regions." *Cell*, vol. 131, no. 2, 2007, pp. 391–404., doi:10.1016/j.cell.2007.09.018.

Chaudhury, Dipesh, et al. "Rapid Regulation of Depression-Related Behaviours by Control of Midbrain Dopamine Neurons." *Nature*, vol. 493, no. 7433, 2012, pp. 532–536., doi:10.1038/nature11713.

Heshmati, Mitra, et al. "Cell-Type-Specific Role for Nucleus Accumbens Neuroligin-2 in Depression and Stress Susceptibility." *Proceedings of the National Academy of Sciences*, vol. 115, no. 5, 2018, pp. 1111–1116., doi:10.1073/pnas.1719014115.

Tian, Guo-Feng, et al. "An Astrocytic Basis of Epilepsy." *Nature Medicine*, vol. 11, no. 9, 2005, pp. 973–981., doi:10.1038/nm1277.

Tsacopoulos, M, and PJ Magistretti. "Metabolic Coupling between Glia and Neurons." *The Journal of Neuroscience*, vol. 16, no. 3, 1996, pp. 877–885., doi:10.1523/jneurosci.16-03-00877.1996.

Janzer, Robert C., and Martin C. Raff. "Astrocytes Induce Blood–Brain Barrier Properties in Endothelial Cells." *Nature*, vol. 325, no. 6101, 1987, pp. 253–257., doi:10.1038/325253a0.

Parpura, Vladimir, and Alexei Verkhratsky. "Homeostatic Function of Astrocytes: Ca2+ and Na+ Signalling." *Translational Neuroscience*, vol. 3, no. 4, 2012, doi:10.2478/s13380-012-0040-y.

Haim, Lucile Ben, and David H. Rowitch. "Functional Diversity of Astrocytes in Neural Circuit Regulation." *Nature Reviews Neuroscience*, vol. 18, no. 1, 2016, pp. 31–41., doi:10.1038/nrn.2016.159.

Nagai, Jun, et al. "Hyperactivity with Disrupted Attention by Activation of an Astrocyte Synaptogenic Cue." *Cell*, vol. 177, no. 5, 2019, doi:10.1016/j.cell.2019.03.019.

Panatier, Aude, et al. "Astrocytes Are Endogenous Regulators of Basal Transmission at Central Synapses." *Cell*, vol. 146, no. 5, 2011, pp. 785–798., doi:10.1016/j.cell.2011.07.022.

Perez-Alvarez, A., et al. "Structural and Functional Plasticity of Astrocyte Processes and Dendritic Spine Inter-

actions." *Journal of Neuroscience*, vol. 34, no. 38, 2014, pp. 12738–12744., doi:10.1523/jneurosci.2401-14.2014.

Guerra-Gomes, Sónia, et al. "The Role of Astrocytic Calcium Signaling in the Aged Prefrontal Cortex." *Frontiers in Cellular Neuroscience*, vol. 12, 2018, doi:10.3389/fncel.2018.00379.

Fiacco, Todd A., and Ken D. McCarthy. "Multiple Lines of Evidence Indicate That Gliotransmission Does Not Occur under Physiological Conditions." *The Journal of Neuroscience*, vol. 38, no. 1, 2018, pp. 3–13., doi:10.1523/jneurosci.0016-17.2017.

Savtchouk, Iaroslav, and Andrea Volterra. "Gliotransmission: Beyond Black-and-White." *The Journal of Neuroscience*, vol. 38, no. 1, 2018, pp. 14–25., doi:10.1523/jneurosci.0017-17.2017.

Adamsky, Adar, et al. "Astrocytic Activation Generates De Novo Neuronal Potentiation and Memory Enhancement." *Cell*, vol. 174, no. 1, 2018, doi:10.1016/j.cell.2018.05.002.

Cao, Xiong, et al. "Astrocyte-Derived ATP Modulates Depressive-like Behaviors." *Nature Medicine*, vol. 19, no. 6, 2013, pp. 773–777., doi:10.1038/nm.3162.

Martin-Fernandez, Mario, et al. "Synapse-Specific Astrocyte Gating of Amygdala-Related Behavior." *Nature Neuroscience*, vol. 20, no. 11, 2017, pp. 1540–1548., doi:10.1038/nn.4649.

Nam, Min-Ho, et al. "Activation of Astrocytic μ-Opioid Receptor Causes Conditioned Place Preference." *Cell Reports*, vol. 28, no. 5, 2019, doi:10.1016/j.celrep.2019.06.071.

Bernard, R, et al. "Altered Expression of Glutamate Signaling, Growth Factor, and Glia Genes in the Locus Coeruleus of Patients with Major Depression." *Molecular Psychiatry*, vol. 16, no. 6, 2010, pp. 634–646., doi:10.1038/mp.2010.44.

Bowley, Michael P, et al. "Low Glial Numbers in the Amygdala in Major Depressive Disorder." *Biological Psychiatry*, vol. 52, no. 5, 2002, pp. 404–412., doi:10.1016/s0006-3223(02)01404-x.

Chandley, Michelle, et al. "Gene Expression Deficits in Pontine Locus Coeruleus Astrocytes in Men with Major

Depressive Disorder." *Journal of Psychiatry & Neuroscience*, vol. 38, no. 4, 2013, pp. 276–284., doi:10.1503/jpn.120110.

Choudary, P. V., et al. "Altered Cortical Glutamatergic and GABAergic Signal Transmission with Glial Involvement in Depression." *Proceedings of the National Academy of Sciences*, vol. 102, no. 43, 2005, pp. 15653–15658., doi:10.1073/pnas.0507901102.

Cotter, D. "Reduced Neuronal Size and Glial Cell Density in Area 9 of the Dorsolateral Prefrontal Cortex in Subjects with Major Depressive Disorder." *Cerebral Cortex*, vol. 12, no. 4, 2002, pp. 386–394., doi:10.1093/cercor/12.4.386.

Ernst, Carl, et al. "Dysfunction of Astrocyte Connexins 30 and 43 in Dorsal Lateral Prefrontal Cortex of Suicide Completers." *Biological Psychiatry*, vol. 70, no. 4, 2011, pp. 312–319., doi:10.1016/j.biopsych.2011.03.038.

Klempan, T A, et al. "Altered Expression of Genes Involved in ATP Biosynthesis and GABAergic Neurotransmission in the Ventral Prefrontal Cortex of Suicides with and without Major Depression." *Molecular Psychiatry*, vol. 14, no. 2, 2007, pp. 175–189., doi:10.1038/sj.mp.4002110.

Miguel-Hidalgo, José Javier, et al. "Reduced Connexin 43 Immunolabeling in the Orbitofrontal Cortex in Alcohol Dependence and Depression." *Journal of Psychiatric Research*, vol. 55, 2014, pp. 101–109., doi:10.1016/j.jpsychires.2014.04.007.

Rajkowska, Grazyna, et al. "Morphometric Evidence for Neuronal and Glial Prefrontal Cell Pathology in Major Depression." *Biological Psychiatry*, vol. 45, no. 9, 1999, pp. 1085–1098., doi:10.1016/s0006-3223(99)00041-4.

Altshuler, Lori L, et al. "Amygdala Astrocyte Reduction in Subjects with Major Depressive Disorder but Not Bipolar Disorder." *Bipolar Disorders*, vol. 12, no. 5, 2010, pp. 541–549., doi:10.1111/j.1399-5618.2010.00838.x.

Miguel-Hidalgo, José Javier, et al. "Glial and Glutamatergic Markers in Depression, Alcoholism, and Their

Comorbidity." *Journal of Affective Disorders*, vol. 127, no. 1-3, 2010, pp. 230–240., doi:10.1016/j.jad.2010.06.003.

Müller, Marianne B., et al. "Neither Major Depression nor Glucocorticoid Treatment Affects the Cellular Integrity of the Human Hippocampus." *European Journal of Neuroscience*, vol. 14, no. 10, 2001, pp. 1603–1612., doi:10.1046/j.0953-816x.2001.01784.x.

Torres-Platas, S G, et al. "Glial Fibrillary Acidic Protein Is Differentially Expressed across Cortical and Subcortical Regions in Healthy Brains and Downregulated in the Thalamus and Caudate Nucleus of Depressed Suicides." *Molecular Psychiatry*, vol. 21, no. 4, 2015, pp. 509–515., doi:10.1038/mp.2015.65.

Stockmeier, Craig A., et al. "Cellular Changes in the Postmortem Hippocampus in Major Depression." *Biological Psychiatry*, vol. 56, no. 9, 2004, pp. 640–650., doi:10.1016/j.biopsych.2004.08.022.

Torres-Platas, Susana G, et al. "Astrocytic Hypertrophy in Anterior Cingulate White Matter of Depressed Suicides." *Neuropsychopharmacology*, vol. 36, no. 13, 2011, pp. 2650–2658., doi:10.1038/npp.2011.154.

Banasr, Mounira, and Ronald S. Duman. "Glial Loss in the Prefrontal Cortex Is Sufficient to Induce Depressive-like Behaviors." *Biological Psychiatry*, vol. 64, no. 10, 2008, pp. 863–870., doi:10.1016/j.biopsych.2008.06.008.

Leng, Lige, et al. "Menin Deficiency Leads to Depressive-like Behaviors in Mice by Modulating Astrocyte-Mediated Neuroinflammation." *Neuron*, vol. 100, no. 3, 2018, doi:10.1016/j.neuron.2018.08.031.

Lee, Hyosang, et al. "Scalable Control of Mounting and Attack by Esr1+ Neurons in the Ventromedial Hypothalamus." *Nature*, vol. 509, no. 7502, 2014, pp. 627–632., doi:10.1038/nature13169.

Shen, Chen-Jie, et al. "Cannabinoid CB1 Receptors in the Amygdalar Cholecystokinin Glutamatergic Afferents to Nucleus Accumbens Modulate Depressive-like Behavior." *Nature Medicine*, vol. 25, no. 2, 2019, pp. 337–349., doi:10.1038/s41591-018-0299-9.

Cryan, John F., et al. "Assessing Antidepressant Activity in Rodents: Recent Developments and Future Needs." *Trends in Pharmacological Sciences*, vol. 23, no. 5, 2002, pp. 238–245., doi:10.1016/s0165-

6147(02)02017-5.

Rygula, Rafal, et al. “Citalopram Counteracts Depressive-like Symptoms Evoked by Chronic Social Stress in Rats.” *Behavioural Pharmacology*, vol. 17, no. 1, 2006, pp. 19–29., doi:10.1097/01.fbp.0000186631.53851.71.

Schiweck, Juliane, et al. “Important Shapeshifter: Mechanisms Allowing Astrocytes to Respond to the Changing Nervous System During Development, Injury and Disease.” *Frontiers in Cellular Neuroscience*, vol. 12, 2018, doi:10.3389/fncel.2018.00261.

Sun, Wei, et al. “SOX9 Is an Astrocyte-Specific Nuclear Marker in the Adult Brain Outside the Neurogenic Regions.” *The Journal of Neuroscience*, vol. 37, no. 17, 2017, pp. 4493–4507., doi:10.1523/jneurosci.3199-16.2017.

Naskar, Saptarnab, and Sumantra Chattarji. “Stress Elicits Contrasting Effects on the Structure and Number of Astrocytes in the Amygdala versus Hippocampus.” *Eneuro*, vol. 6, no. 1, 2019, doi:10.1523/eneuro.0338-18.2019.

Agulhon, Cendra, et al. “What Is the Role of Astrocyte Calcium in Neurophysiology?” *Neuron*, vol. 59, no. 6, 2008, pp. 932–946., doi:10.1016/j.neuron.2008.09.004.

Araque, Alfonso, et al. “Gliotransmitters Travel in Time and Space.” *Neuron*, vol. 81, no. 4, 2014, pp. 728–739., doi:10.1016/j.neuron.2014.02.007.

Griffin, Jarred M., et al. “Astrocyte-Selective AAV Gene Therapy through the Endogenous GFAP Promoter Results in Robust Transduction in the Rat Spinal Cord Following Injury.” *Gene Therapy*, vol. 26, no. 5, 2019, pp. 198–210., doi:10.1038/s41434-019-0075-6.

Yu, Xinzhu, et al. “Reducing Astrocyte Calcium Signaling In Vivo Alters Striatal Microcircuits and Causes Repetitive Behavior.” *Neuron*, vol. 99, no. 6, 2018, doi:10.1016/j.neuron.2018.08.015.

Erickson, E. K., et al. “Cortical Astrocytes Regulate Ethanol Consumption and Intoxication in Mice.” *Neuropsychopharmacology*, vol. 46, no. 3, 2020, pp. 500–508., doi:10.1038/s41386-020-0721-0.

Matsuda, Seiji, et al. “Persistent c-Fos Expression in the Brains of Mice with Chronic Social Stress.” *Neuroscience Research*, vol. 26, no. 2, 1996, pp. 157–170., doi:10.1016/s0168-0102(96)01088-7.

Numa, Chisato, et al. “Social Defeat Stress-Specific Increase in c-Fos Expression in the Extended Amygdala in Mice: Involvement of Dopamine D1 Receptor in the Medial Prefrontal Cortex.” *Scientific Reports*, vol. 9, no. 1, 2019, doi:10.1038/s41598-019-52997-7.

Hol, Elly M, and Milos Pekny. “Glial Fibrillary Acidic Protein (GFAP) and the Astrocyte Intermediate Filament System in Diseases of the Central Nervous System.” *Current Opinion in Cell Biology*, vol. 32, 2015, pp. 121–130., doi:10.1016/j.ceb.2015.02.004.

Shigetomi, Eiji, et al. “Aberrant Calcium Signals in Reactive Astrocytes: A Key Process in Neurological Disorders.” *International Journal of Molecular Sciences*, vol. 20, no. 4, 2019, p. 996., doi:10.3390/ijms20040996.

Cui, Wanpeng, et al. “Glial Dysfunction in the Mouse Habenula Causes Depressive-Like Behaviors and Sleep Disturbance.” *The Journal of Neuroscience*, vol. 34, no. 49, 2014, pp. 16273–16285., doi:10.1523/jneurosci.1465-14.2014.

Cui, Yihui, et al. “Astroglial Kir4.1 in the Lateral Habenula Drives Neuronal Bursts in Depression.” *Nature*, vol. 554, no. 7692, 2018, pp. 323–327., doi:10.1038/nature25752.

Anthony, Todd E., et al. “Control of Stress-Induced Persistent Anxiety by an Extra-Amygdala Septohypothalamic Circuit.” *Cell*, vol. 156, no. 3, 2014, pp. 522–536., doi:10.1016/j.cell.2013.12.040.

Parfitt, Gustavo Morrone, et al. “Bidirectional Control of Anxiety-Related Behaviors in Mice: Role of Inputs Arising from the Ventral Hippocampus to the Lateral Septum and Medial Prefrontal Cortex.” *Neuropsychopharmacology*, vol. 42, no. 8, 2017, pp. 1715–1728., doi:10.1038/npp.2017.56.

Sheehan, Teige P, et al. “Regulation of Affect by the Lateral Septum: Implications for Neuropsychiatry.” *Brain Research Reviews*, vol. 46, no. 1, 2004, pp. 71–117., doi:10.1016/j.brainresrev.2004.04.009.

Guzmán, Yomayra F, et al. “Fear-Enhancing Effects of Septal Oxytocin Receptors.” *Nature Neuroscience*, vol.

16, no. 9, 2013, pp. 1185–1187., doi:10.1038/nn.3465.

Terrill, Sarah J., et al. “Lateral Septum Growth Hormone Secretagogue Receptor Affects Food Intake and Motivation for Sucrose Reinforcement.” *American Journal of Physiology-Regulatory, Integrative and Comparative Physiology*, vol. 315, no. 1, 2018, doi:10.1152/ajpregu.00339.2017.

Besnard, Antoine, et al. “Dorsolateral Septum Somatostatin Interneurons Gate Mobility to Calibrate Context-Specific Behavioral Fear Responses.” *Nature Neuroscience*, vol. 22, no. 3, 2019, pp. 436–446., doi:10.1038/s41593-018-0330-y.

Ebner, Karl, et al. “Neurokinin 1 Receptor Antagonism Promotes Active Stress Coping Via Enhanced Septal 5-HT Transmission.” *Neuropsychopharmacology*, vol. 33, no. 8, 2007, pp. 1929–1941., doi:10.1038/sj.npp.1301594.

Mirrione, Martine M., et al. “Increased Metabolic Activity in the Septum and Habenula during Stress Is Linked to Subsequent Expression of Learned Helplessness Behavior.” *Frontiers in Human Neuroscience*, vol. 8, 2014, doi:10.3389/fnhum.2014.00029.

Singewald, Georg M, et al. “The Modulatory Role of the Lateral Septum on Neuroendocrine and Behavioral Stress Responses.” *Neuropsychopharmacology*, vol. 36, no. 4, 2010, pp. 793–804., doi:10.1038/npp.2010.213.

Wang, Dan, et al. “Regulation of Depression-Related Behaviors by GABAergic Neurons in the Lateral Septum through Periaqueductal Gray Neuronal Projections.” *Journal of Psychiatric Research*, vol. 137, 2021, pp. 202–214., doi:10.1016/j.jpsychires.2021.02.043.

Brady, Joseph V., and Walle J. Nauta. “Subcortical Mechanisms in Emotional Behavior: the Duration of Affective Changes Following Septal and Habenular Lesions in the Albino Rat.” *Journal of Comparative and Physiological Psychology*, vol. 48, no. 5, 1955, pp. 412–420., doi:10.1037/h0046406.

Pesold, Christine, and Dallas Treit. “The Neuroanatomical Specificity of the Anxiolytic Effects Ofintra-Septal Infusions of Midazolam.” *Brain Research*, vol. 710, no. 1-2, 1996, pp. 161–168., doi:10.1016/0006-

8993(95)01359-8.

Radulovic, Jelena, et al. “Modulation of Learning and Anxiety by Corticotropin-Releasing Factor (CRF) and Stress: Differential Roles of CRF Receptors 1 and 2.” *The Journal of Neuroscience*, vol. 19, no. 12, 1999, pp. 5016–5025., doi:10.1523/jneurosci.19-12-05016.1999.

Henry, B. “The Effect of Lateral Septum Corticotropin-Releasing Factor Receptor 2 Activation on Anxiety Is Modulated by Stress.” *Journal of Neuroscience*, vol. 26, no. 36, 2006, pp. 9142–9152., doi:10.1523/jneurosci.1494-06.2006.

Parfitt, Gustavo Morrone, et al. “Bidirectional Control of Anxiety-Related Behaviors in Mice: Role of Inputs Arising from the Ventral Hippocampus to the Lateral Septum and Medial Prefrontal Cortex.” *Neuro-psychopharmacology*, vol. 42, no. 8, 2017, pp. 1715–1728., doi:10.1038/npp.2017.56.

요 약 문

뇌 측면 중격 지역 내 성상교세포에 의한 스트레스 유발 행동의 조절

만성적인 스트레스는 불안, 우울증 및 기타 정신 장애와 관련되어 있습니다. 이에 대해 스트레스에 대한 행동 반응을 매개하는 신경 메커니즘에 대한 연구가 주로 진행되어져 왔지만, 최근 성상교세포 연구에 대한 관심이 높아지고 있습니다. 성상교세포는 신경세포에 대한 항상성 지원을 제공할 뿐만 아니라 신경세포와 상호 작용하여 행동 조절에 중요한 역할을 합니다. 그러나, 성상교세포의 다양한 기능에도 불구하고, 스트레스 관련 행동에서 성상교세포의 역할에 대한 연구는 소수의 뇌 지역에서만 진행되었습니다. 우울증 연구에 사용되는 동물 모델인 만성 사회적 패배 스트레스를 사용하여, 뇌 측면 중격 지역의 성상교세포가 스트레스에 대해 지연된 반응을 보인다는 것을 발견했습니다. 반응성 성상교세포의 특징을 나타내는 분자 및 형태학적 변화가 만성 사회적 패배 스트레스 이후 측면 중격 지역에서 관찰되었습니다. 측면 중격 지역의 성상교세포에서 Gq 경로를 활성화하여 성상교세포의 칼슘 신호를 높이는 것은 성상교세포 및 신경세포의 활동을 증가시켰고, 대조군 쥐의 행동에는 영향을 주지 않는 역치 이하 스트레스가 주어졌을 때 우울 및 불안 관련 행동을 유발했습니다. 반대로, 측면 중격 지역 성상교세포에서 칼슘 신호를 감소시키면 급성 스트레스에 의해 나타나는 신경세포의 활성이 차단되었습니다. 특히, 측면 중격 지역의 성상교세포 특이적 억제는 만성 사회적 패배 스트레스 후에 항우울제 유사 효과를 나타냈습니다. 따라서 본 논문은 측면 중격 지역 내 성상교세포가 스트레스로 인해 유발되는 행동들을 조절하고 우울증 치료를 위한 새로운 접근법을 제시하는 데 기여할 수 있다는 것을 보여주고 있습니다.

핵심어: 스트레스, 성상교세포, 측면 중격, 우울증, 불안증, 사회적 패배, 화학유전학, cFos